SILICA PARTICLES FOR HYDROPHOBIC DRUG DELIVERY FROM SILICONE HYDROGELS

SILICA PARTICLES FOR HYDROPHOBIC DRUG DELIVERY FROM SILICONE HYDROGELS

By

MICHELLE D. FERNANDES, B.Sc.

A Thesis Submitted to

the School of Graduate Studies

in Partial Fulfillment of the Requirements for the Degree

Master of Applied Science

McMaster University

MASTER OF APPLIED SCIENCE (2013) McMaster University

(Chemical Engineering) Hamilton, Ontario

TITLE: Silica particles for hydrophobic drug delivery from silicone hydrogels

AUTHOR: Michelle D. Fernandes, B.Sc. (McMaster University)

SUPERVISOR: Professor H. Sheardown

NUMBER OF PAGES: 104

ABSTRACT

Topical administration of therapeutic eye drops is currently the most employed method of drug delivery for treatment of various ocular conditions. The poor drug bioavailability with this method of delivery requires frequent administration and results in low patient compliance. Drug eluting contact lenses have been proposed as a means to overcome the challenges associated with topical drug delivery due to the ability to increase drug residence time on the ocular surface and consequently increase corneal absorption. In this study, silica particles were prepared using microemulsion polymerization, and were embedded into a model silicone hydrogel consisting hydroxyethylmethacrylate (HEMA) monomer and a hydroxylated silicone monomer. Silica particles were specifically selected as the drug-containing particle system for loading into a silicone hydrogel to observe whether better control over the rate of drug release was possible by loading the hydrophobic drug in the silicone domain via the use of silica particles. Although similar dexamethasone release profiles were observed for hydrogels incorporated with suspensions prepared with or without silica shell precursors, transmission electron micrographs of these hydrogels indicate particle localization in silicone domains for suspensions prepared with silica precursors. This result is promising, and optimization of the drug-containing silica particle synthesis formulation may potentially allow for control over the drug release profile.

ACKNOWLEDGEMENTS

First, I want to thank my supervisor Dr. Heather Sheardown. Heather, thank you for providing me with the opportunity and freedom to explore my research. As a result, I learnt an incredible amount about the scientific process that extends well beyond my direct research. Dr. Todd Hoare, Dr. Kathryn Grandfield, and Dr. Lyndon Jones, thank you for the helpful discussions.

I also want to thank Nicole Mangiacotte, who worked with me for a summer, for all of her hard work. To the members of the Sheardown group especially Lina Liu, Jafar Mazumder, Stefan Paterson, Giuliano Guidi, and Myrto Korogiannaki, as well as members of other research groups, Daryl Sivakumaran, Zuohe (Kevin) Wang, Songtao Yang, Rabia Mateen, and Marlena Whinton, thank you for the helpful discussions. Thank you also to Marcia Reid at the Health Sciences Centre electron microscopy facility for helpful discussions, transmission electron microscopy sample preparation, and for imaging some of the samples.

To all of my friends in the department, especially Hongyu Lu and Carla Abarca, thank you for making my time here all the more enjoyable!

Mom and Dad, you are the most amazing people I know. I could not have asked for better parents. Thank you for giving me so much. Sis, you are my gold standard for everything. Sis and Jimmy, thank you for all of your support.

TABLE OF CONTENTS

ABSTRACT……iii

ACKNOWLEDGEMENTS……iv

TABLE OF CONTENTS……v

LIST OF FIGURES viii

LIST OF TABLES xi

LIST OF ABBREVIATIONS xii

DECLARATION OF ACADEMIC ACHIEVEMENT……..xiii

1. INTRODUCTION 1

2. LITERATURE REVIEW 5

2.1 Glaucoma 5

2.2 Current treatment options for glaucoma and challenges 7

2.3 Hydrogel contact lenses for controlled drug delivery 10

2.3.1 Silicone hydrogels as a therapeutic contact lens 12

2.4 Methods of loading hydrophobic drugs into hydrogels 14

2.4.1 Soaking contact lenses in drug solution 14

2.4.2 Direct entrapment 19

2.4.3 Cyclodextrins and surface functionalization with liposomes 21

2.4.4 Particles for controlled drug delivery 22

2.5 Objectives of current research 34

3. MATERIALS AND METHODS 37

3.1 Reagents 37

3.2 Miniemulsion for drug-containing silica particle synthesis 39

3.2.1 Particle characterization by dynamic light scattering (DLS) 41

3.2.2 Particle stability in phosphate buffered saline (PBS) 41

3.2.3 Effect of acetazolamide loading on particle diameter 43

3.3 Microemulsion for dexamethasone-containing silica particle synthesis 43

3.3.1 Dexamethasone partitioning in oil/deionized water 43

3.3.2 Particle synthesis by microemulsion polymerization technique 44

3.4 Incorporation of dexamethasone-containing silica particles in a model silicone hydrogel 46

3.4.1 Water tolerance of hydrophilic and silicone monomers 46

3.4.2 Synthesis of HEMA/TRIS-OH silicone hydrogels containing dexamethasone-loaded particles 47

3.4.3 Characterization of hydrogels 48

3.5 Dexamethasone release study 49

4. RESULTS AND DISCUSSION 51

4.1 Optimization of silica particle size 51

4.2 Factors affecting drug-loaded silica particle stability in PBS for particles prepared by miniemulsion technique 53

4.2.1 Effect of polymer adsorption on particle stability in PBS for atropine-containing particles 56

4.2.2 Effect of surfactant content on particle stability in PBS for acetazolamide-containing particles 58

4.3 Effect of acetazolamide loading on particle diameter 62

4.4 Dexamethasone partitioning in oil/water for selection of internal phase oil for microemulsions 63

4.5 Dexamethasone-loaded silica nanoparticle synthesis prepared by the microemulsion technique 64

4.5.1 Effect of dexamethasone loading 64

4.5.2 Effect of silica shell precursors 65

4.6 Characterization of HEMA/TRIS-OH silicone hydrogels embedded with dexamethasone-loaded particles 66

4.6.1 Equilibrium water content 68

4.6.2 Transparency 70

4.6.3 Transmission electron microscopy (TEM) for particle visualization 73

4.7 Dexamethasone release from HEMA/TRIS-OH silicone hydrogels embedded with dexamethasone-loaded silica particles 81

4.7.1 Effect of dexamethasone loading 82

4.7.2 Effect of silica shell precursors 83

4.8 Mechanism of drug release for hydrogels embedded with drug-containing particles

5. CONCLUSIONS AND RECOMMENDATIONS 89

5.1 Conclusions 89

5.2 Recommendations for future work 91

6. REFERENCES 93

Appendix A 102

Appendix B 103

LIST OF FIGURES

Chapter 2

Figure 2.1. (A) open-angle and **(B)** closed-angle glaucoma…….. 5

Figure 2.2. Schematic of pulsatile and controlled drug release profiles…… 9

Figure 2.3. Drug released from a contact lens enters the post-lens tear film and its residence time on the cornea is increased compared to topical administration of the drug…….. 12

Figure 2.4. Hydrolysis and condensation reactions between TEOS and OTMS……... 28

Figure 2.5. Schematic of oil-filled silica nanocapsule formation with OTMS and TMOS as silica shell precursors…….. 31

Chapter 3

Figure 3.1. Chemical structure of acetazolamide…… 37

Figure 3.2. Chemical structure of atropine…… 38

Figure 3.3. Chemical structure of dexamethasone……. 39

Figure 3.4. Synthesis of silica particles by miniemulsion polymerization technique…… 40

Figure 3.5. (A). MATO and **(B).** TEOS……... 45

Figure 3.6. Synthesis of silica nanoparticles by microemulsion polymerization technique……... 46

Chapter 4

Figure 4.1. Effect of sonication intensity on particle diameter……..... 52

Figure 4.2. Effect of sonication duration on particle diameter……... 53

Figure 4.3. Effect of aging step pH on particle diameter……..... 55

Figure 4.4. Atropine-containing particle stability in PBS for particles prepared at various aging step pH values……..... 55

Figure 4.5. Stability of empty and atropine-containing silica particles incubated with 0, 10, 50, 100, 500, and 1000 mg/mL (w/v) 4.4 kDa DMS-PEO copolymer approximately 0 and 1 h after addition to PBS……. 57

Figure 4.6. Acetazolamide-containing particle stability in PBS for particles prepared using various amounts of SDS (% wt SDS/wt surfactant)…….. 61

Figure 4.7. Effect of amount of SDS (% wt SDS/wt surfactant) on particle diameter…… 62

Figure 4.8 (A). TRIS and **(B)** TRIS-OH……. 68

Figure 4.9. % transmittance for HEMA/TRIS-OH gels embedded with silica nanoparticles containing 0, 1x, or 2x dexamethasone……... 71

Figure 4.10. % transmittance for HEMA/TRIS-OH gels embedded with particles prepared with and without silica shell precursors and with or without dexamethasone…… 72

Figure 4.11. % transmittance for HEMA/TRIS-OH disks and MATO/D disks…….. 73
.

Figure 4.12. TEM micrographs of HEMA/TRIS-OH (90:10) hydrogel embedded with dexamethasone-containing particles with MATO as silica shell precursor……..... 76

Figure 4.13. TEM micrographs of HEMA/TRIS-OH (90:10) hydrogel embedded with dexamethasone-containing particles with TEOS as silica shell precursor……..... 78

Figure 4.14. TEM micrographs of dexamethasone-containing nanoparticles with **(A)** MATO silica shell precursor, **(B)** TEOS silica shell precursor, and **(C)** no silica shell precursor……..…. 81

Figure 4.15. Dexamethasone release in PBS at 34°C from silica nanoparticles containing 1x and 2x dexamethasone…… 82

Figure 4.16. Dexamethasone release into PBS at 34°C from HEMA/TRIS-OH disks embedded with particles synthesized with MATO, TEOS, or no shell precursor……. 84

Appendix B

Figure A1. Calibration curve of atropine in PBS……... 103

Figure A2. Calibration curve of acetazolamide in PBS…… 103

Figure (A3). TEM micrograph of HEMA and **(A4).** HEMA/dH_2O hydrogel at 10,000x magnification…… 104

LIST OF TABLES

Chapter 3

Table 3.1. Model drugs and their logP values……... 39

Chapter 4

Table 4.1. Electrophoretic mobility of empty and atropine-containing silica particles incubated with increasing concentrations of DMS-PEO copolymer……. 58

Table 4.2. SDS amounts and corresponding vial numbers……. 61

Table 4.3. Effect of acetazolamide loading on particle diameter…… 63

Table 4.4. Concentration of dexamethasone in water and oils……... 64

Table 4.5. Effect of dexamethasone loading on particle diameter…… 65

Table 4.6. Particle diameters of particles prepared with and without silica shell precursors……... 65

Table 4.7. Equilibrium water content for HEMA/TRIS-OH gels embedded with silica nanoparticles containing 0, 1x, or 2x dexamethasone……... 69

Table 4.8. Equilibrium water content for HEMA/TRIS-OH disks embedded with particles prepared with and without silica shell precursors and with or without dexamethasone……. 69

Table 4.9. Equilibrium water content for HEMA/TRIS-OH disks and MATO/D disks……. 70

Appendix A

Table A1. Reagents and source…….. 102

Table A2. Recipe for 1x PBS…… 102

LIST OF ABBREVIATIONS

ANOVA	Analysis of variance
DLS	Dynamic light scattering
DMA	*N,N*-dimethylacrylamide
DMS-PEO	Dimethylsiloxane-polyethylene oxide
DXM	Dexamethasone
EGDMA	Ethylene glycol dimethacrylate
EWC	Equilibrium water content
HEMA	2-Hydroxyethylmethacrylate
HPLC	High performance liquid chromatography
IOP	Intraocular pressure
MATO	Methacryloxypropyltriethoxysilane
NaCl	Sodium chloride
NaOH	Sodium hydroxide
OTMS	Octadecyltrimethoxysilane
PBS	Phosphate buffered saline
PGT	Propoxylated glyceryl triacrylate
PLGA	Polylactic-co-glycolic acid
PVA	Polyvinyl alcohol
SD	Standard deviation
SDS	Sodium dodecyl sulphate
TEM	Transmission electron microscopy
TEOS	Tetraethoxysilane
TMOS	Tetramethoxysiloxane
TRIS	methacryloxypropyltris(tri-methylsiloxy)silane
TRIS-OH	3-(3-methacryloxy-2-hydroxypropoxy)propylbis(trimethylsiloxy)methylsilane)
UV	Ultraviolet

DECLARATION OF ACADEMIC ACHIEVEMENT

This thesis was written solely by Michelle D. Fernandes. Design of all experiments and data analysis was done by Michelle D. Fernandes. Nicole Mangiacotte synthesized particles, performed particle size measurements, and stability studies for the following studies: optimization of silica particle size, effect of the aging step pH and surfactant content on particle stability in phosphate buffered saline, and the effect of acetazolamide loading on particle diameter. Nicole Mangiacotte also prepared dilutions and took ultraviolet absorbance measurements for preparation of the atropine and acetazolamide calibration curves. Marcia Reid at the Health Sciences Centre electron microscopy facility prepared hydrogel and particle suspension samples, synthesized by Michelle D. Fernandes, for transmission electron microscopy, and imaged particle suspension samples, and HEMA and HEMA/dH_2O hydrogel samples. All other experiments were conducted by Michelle D. Fernandes.

The ideas for the use of a hydroxylated silicone monomer, and a silica shell precursor containing an acryl group were generated from discussions with Giuliano Guidi and Lina Liu respectively.

1. INTRODUCTION

Glaucoma is a disease that affects more than 400,000 Canadians, and is the second most prevalent cause of vision loss amongst seniors in Canada (The Glaucoma Research Society of Canada, 2013; CNIB, 2013). It has, as a risk factor, the build-up of intraocular pressure (IOP) due to an increase in the production or a decrease in the drainage of the aqueous humour. This elevated IOP, if left untreated, can severely damage the optic nerve and could eventually lead to vision loss. The primary form of disease management is by topical application of ointments or solutions containing therapeutic agents aimed at lowering IOP. The effectiveness of this form of treatment however, relies on patient compliance and on the proper drug administration. Additionally, the short residence time of the solution on the cornea due to spillage of the solution onto the cheek, absorption by the conjunctiva, or drainage to the nasolacrimal duct results in only about 5% of the applied therapeutic agent reaching the intraocular tissues. For some therapeutic formulations, this means the formulation must be applied multiple times daily to achieve the therapeutic dosage. Additionally, the drug that is not absorbed by the cornea may enter systemic circulation and pose side effects. Timolol, a beta-blocker prescribed for glaucoma, can for example, cause deleterious cardiovascular effects (Merck Canada Inc., 2013). There is clearly a need for a drug delivery method that can increase the amount of drug that reaches the intraocular tissue in a manner that is safe and therapeutically effective.

Contact lenses have been investigated as a potential drug delivery vehicle to improve the bioavailability of therapeutic agents for treatment of ocular diseases (Alvarez-Lorenzo et al., 2006). Contact lenses are attractive for drug delivery as these devices can be worn for extended periods of time. Silicone hydrogel contact lenses, with their increased oxygen permeability, can allow for up to 30 days of continuous wear (Montero et al., 2001). When a drug-loaded contact lens is applied to the eye, the drug diffuses out of the hydrogel matrix and enters the post lens tear film, the fluid layer between the contact lens and the cornea. Due to limited mixing between the post lens tear film and the external tear fluid, the residence time of the drug on the cornea is increased (Creech et al., 2001; McNamara et al., 1999). With a drug-loaded contact lens, it is estimated that approximately 50% of the applied drug is absorbed through the cornea, a substantial increase compared with topical application (Li and Chauhan, 2006). Furthermore, this increased corneal absorption also means lesser drug absorption to systemic circulation.

Investigators have explored various methods for loading a drug into a contact lens. The most common method of drug loading is by soaking the lens in a solution containing the drug of interest. The drug release kinetics with this approach mimics the uptake kinetics, therefore control over the release behaviour is limited (Karlgard, 2003a).

Drug-containing particles are an attractive method for loading a hydrophobic drug into a hydrogel. Nanoparticles with an oily hydrophobic core will incorporate a hydrophobic drug. These drug-containing particles may then be loaded into a hydrogel formulation. The presence of particles is expected to act as an additional barrier to drug release as the drug must diffuse out of the particle and then through the hydrogel matrix. Furthermore, although present in the gel formulation during polymerization, the drug is encapsulated within the particle and is protected during polymerization.

Investigators have previously incorporated particle systems within a hydroxyethylmethacrylate (HEMA)-based gel formulaton to prepare hydrogels embedded with drug-containing particles (Gulsen and Chauhan, 2004; Lu et al., 2013). However, few studies have incorporated drug-containing particles in silicone hydrogels (Jung et al., 2013). In the current work, an aqueous suspension of drug-containing silica nanoparticles were added to a silicone hydrogel formulation to prepare silicone hydrogels embedded with drug-containing silica particles. Silica particles were used as it is hypothesized that the silica particles will associate with the silicone domain of the silicone hydrogel matrix and potentially slow the rate of release due to a more limited access of the hydrophobic silicone domains to water channels. A hydroxylated silicone monomer was used to allow for the incorporation of an aqueous particle suspension in a silicone hydrogel formulation. Furthermore, the use of a silica precursor with an acryl group in its chemical structure was used to investigate

whether particle immobilization in the silicone domain via chemical bonding between the acryl group of the silica shell and the silicone monomers of the hydrogel matrix may affect the drug release profile.

2. LITERATURE REVIEW

2.1 Glaucoma

Glaucoma affects over 400,000 Canadians, and 67 million people globally (The Glaucoma Research Society of Canada, 2013). It is a disease that has as a risk factor, increased intraocular pressure (IOP). Elevated IOP may cause damage to the optic nerve, leading to vision loss. While there are different forms of glaucoma, the two main categories are open-angle glaucoma and angle-closure glaucoma. With angle-closure glaucoma, there is closure of the anterior chamber angle. With open-angle glaucoma, the more prevalent form, the anterior chamber angle remains open (**Figure 2.1**).

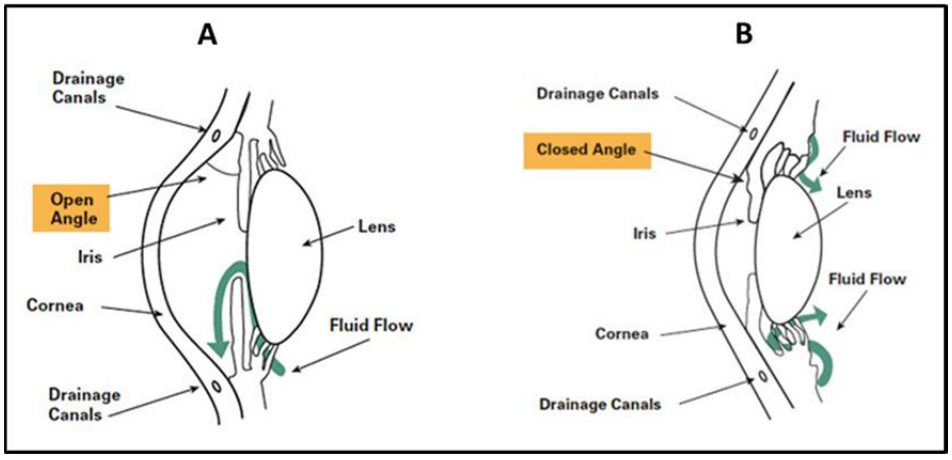

Figure 2.1 (A) open-angle and **(B)** closed-angle glaucoma. Illustrations are adapted from www.glaucoma.org – the website of the Glaucoma Research Foundation in San Francisco, California – and are copyrighted by the Glaucoma Research Foundation.

The risk factors for open-angle glaucoma are advancing age, family history of glaucoma, prior eye trauma, African-American heritage, vasospastic diseases like migraines and Raynaud's phenomena, a reduction in blood circulation to the optic nerve possibly arising from low blood pressure, severe anemia, and a history of blood transfusion (Lee and Higginbotham, 2005; Klein et al., 2004). With angle-closure glaucoma, the aqueous humour cannot flow through the pupil into the anterior chamber. This condition, known as pupiliary block, results in a build-up of pressure behind the iris, forcing it anteriorly and causing subsequent anterior chamber angle closure. Risk factors for angle-closure glaucoma include advancing age, family history of glaucoma, prior eye trauma, Asian heritage, hyperopia, and pseudoexfoliation (Lee and Higginbotham, 2005; Wang *et al*, 2002). With angle-closure glaucoma, the patient may experience a sudden onset of blurred or decreased vision, eye pain and redness, may see halos around lights, have headaches and may experience nausea and vomiting related to an increase in IOP from 30 mm Hg to over 80 mm Hg, where the normal range lies between 10 to 21mm Hg (Lee and Higginbotham, 2005).

An increased intraocular pressure can arise from an increase in aqueous humor production or a decrease in drainage of the aqueous humor. Increased IOP may also occur in patients suffering from uveitis. Although the mechanism by which uveitis leads to increased IOP is not completely understood, the imbalance arising from aqueous humor production and the resistance to outflow

due to inflammation may be responsible for the change in IOP (Siddique et al. 2013). In patients experiencing ocular inflammation, this resistance to outflow may result from a blockage of the trabecular meshwork by inflammatory cells, proteins, and debris, fibrin from the disrupted blood-aqueous barrier, swelling, or dysfunction of the trabecular lamellae or endothelium (Moorthy et al., 1997).

2.2 Current treatment options for glaucoma and challenges

Current glaucoma treatment methods are aimed at lowering IOP. The first line of treatment typically involves topical administration of IOP lowering drugs. There are five main classes of glaucoma drugs; prostaglandin analogues, beta blockers, adrenergic agents, cholinergic drugs, and carbonic anhydrase inhibitors. Currently, prostaglandin analogues are the most effective topical agents for reducing IOP (Eisenberg et al., 2002; Netland et al., 2001; Sherwood and Brandt, 2001; van der Valk et al., 2005). Prostaglandin analogues reduce IOP by increasing aqueous humor outflow. Surgical treatment may also be required for patients whose IOP is not sufficiently lowered, or if the patient experiences progressive worsening of the visual field, progressive damage to the optic disc, or thinning of the retinal nerve fiber layer. Depending on the type of glaucoma, laser surgery including laser trabeculoplasty, and laser iridotomy may be performed. Alternatively surgical intervention including nonpenetrating drainage surgery or trabeculectomy might be done. Iridectomy or iridotomy involves creating an opening in the peripheral iris to allow aqueous flow between the posterior and the anterior chamber (Lee and Higginbotham, 2005).

Cycloablation, is a last resort technique in which aqueous humour production is decreased upon destruction of the ciliary body with a transcleral or intraocular diode Nd:YAG laser cycophotocoagulation or an 810 nm infrared diode laser. This technique however, can increase inflammation, lead to postoperative hypotony, and phthisis bulbi (Siddique et al., 2013).

The majority of drugs aimed at lowering IOP are administered topically. Upon administration of the aqueous drug solution, the drug mixes with the tear solution, and typically only 5% of the drug is absorbed into the cornea (Järvinen et al., 1995; Urtti, 2006). The low percentage of corneal absorption is, in part, due to a low residence time when a topical solution is employed as a means of drug delivery. The human cul-de-sac has a volume of approximately 7 μL and can expand to 30 μL. Upon instillation of a topical solution, the solution volume that does not remain in the cul-de-sac is drained into the nasolacrimal duct, is absorbed by the conjunctiva, or spills onto the cheek upon blinking. Furthermore, the increase in the tear turnover rate that occurs upon instillation of the drop results in almost complete disappearance of the applied drug in the cul-de-sac within five minutes (Law and Lee, 2008). This wasted drug can be problematic if adverse side effects occur when the drug enters the systemic circulation. For instance, timolol, a beta blocker administered for lowering IOP can have deleterious effects on the heart (Merck Canada Inc., 2013). As well, topical administration of drug solutions results in pulsatile drug delivery, whereby upon application of the drug solution there may be an overdose, followed by a short

period during which the therapeutic dose is achieved, and finally there is period of underdosing at which point the topical drug solution would need to be re-administered (Ciolino et al., 2009). **Figure 2.2** shows a schematic of the pulsatile release profile associated with topical administration. An ideal controlled release profile where the drug concentration reaches a level that is constantly within the range of therapeutic effectiveness is also shown. The frequent dosing required to obtain therapeutic effectiveness for some topical solutions can contribute to low patient compliance. Additionally, difficulties in drop application and forgetfulness in regular application of drops are other factors that reduce the efficacy of this drug delivery vehicle (Lacey et al., 2009). There is clearly a need for alternative drug delivery methods that can overcome these challenges.

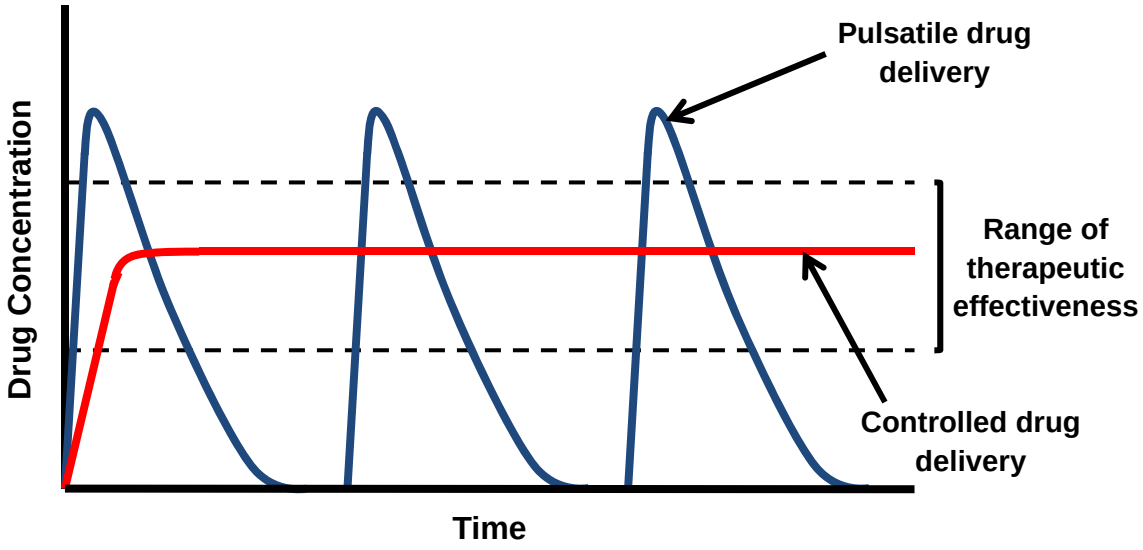

Figure 2.2. Schematic of pulsatile and controlled drug release profiles.

Therefore, in order to increase the residence time of ophthalmic drugs, several alternative methods of drug delivery have been proposed. A particularly

promising method involves *in situ* forming gels that are triggered by pH, temperature, or ions (Ma et al., 2008; Srividya and Cardoza, 2001; Xionga et al., 2011; Ibrahim et al., 1991; Gupta and Vyas, 2010; Katerina et al., 1998; El-Kamel, 2002; Gana et al., 2009; Balasubramaniam, 2003). Other methods of delivery include using formulations containing colloidal particles and collagen shields, punctal plugs, conjunctival inserts, bandage lenses and contact lenses (Le Bourlais, et al., 1998; Vasantha and Panduranga, 1988).

2.3 Hydrogel contact lenses for controlled drug delivery

Contact lenses have been widely touted as a method for increasing the residence time of drugs in the eye. As seen in **Figure 2.3**, with a drug eluting contact lens, once the drug diffuses out of the contact lens into the post lens tear film, located between the contact lens and the cornea, the residence time is increased to 30 minutes compared to two minutes with topical application of the drug (Le Bourlais et al.,1998; Creech et al., 2001; McNamara et al., 1999). Therefore, therapeutic lenses with the potential to release the drug over a prolonged period of time, may remove the need for frequent patient administration. In addition, drug delivery via contact lenses is expected to reduce drug wastage from improper administration of the eye drop, drainage into the nasolacrymal duct, and spillage onto the cheek. With the reduced amount of drug entering systemic circulation, side effects associated with the drug will also be minimized. Furthermore, with prolonged drug delivery to the post lens tear film, more drug may be absorbed through the cornea. Based on mathematical

models of soaked contacted lenses for instance, it is estimated that approximately 50% of the drug delivered via contact lenses reaches the cornea compared to an estimated 5% that reaches the internal ocular structures following eyedrop administration (Li and Chauhan, 2006). Currently, therapeutic lenses are a standard method of treatment for a variety of anterior segment conditions. Indications include relief of pain and discomfort, and assistance in the healing of injured or diseased ocular tissue (Ambroziak et al., 2004). The potential for contact lenses as drug delivery vehicles for posterior segment conditions has also been demonstrated in a rabbit model, in which detectable amounts of prednisolone, beclomethasone, and ranibizumab released from lidofilcon hydrogel contact lenses were measured in posterior segment tissues (Schultz et al., 2011).

Hydrogels are an extremely attractive biomaterial for drug delivery (Hoare and Kohane, 2008). These three-dimensional, cross-linked networks consisting of water soluble polymers can absorb large quantities of water. Their high water content, porosity, and physiochemical similarity to the native extracellular matrix contribute to the biocompatibility of these materials. In terms of drug delivery, the high water content of hydrogels poses a challenge; hydrophilic drugs diffuse rapidly through the water filled channels while loading of hydrophobic drugs can be problematic.

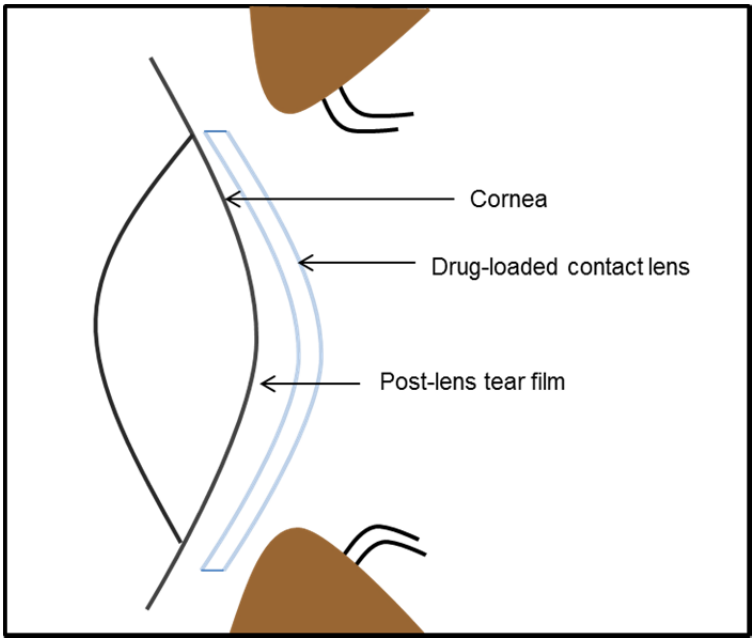

Figure 2.3. Drug released from a contact lens enters the post-lens tear film and its residence time on the cornea is increased compared to topical administration of the drug. Adapted from Kim and Chauhan, 2008.

2.3.1 Silicone hydrogels as a therapeutic contact lens

Silicone hydrogel contact lenses are becoming increasingly popular due to their increased oxygen permeability. Conventional hydrogel lenses are composed of monomers such as N-vinyl pyrrolidone (NVP), methacrylic acid, and 2-hydroxyethyl methacrylate that attract and bind water within the polymeric matrix (Tighe, 2004). In addition to water binding monomers, silicone hydrogel lenses consist of silicone containing monomers or macromers, which serve to increase the oxygen permeability of the material. Oxygen permeability (Dk) is a product of diffusion (D) and solubility (k). Oxygen is more soluble in water than polymethylmethacrylate and more soluble in silicone rubber than in water. The increased solubility in silicone rubber is due to silicon-oxygen and silicon-carbon

bonds. With conventional hydrogels, the low oxygen solubility in the carbon backbone means the main mode of oxygen transport is through the aqueous phase. In silicone hydrogels, on the other hand, the high solubility in the silicone segments means that oxygen permeability increases with the proportion of silicone polymer in the gel. At an equilibrium water content (EWC) of approximately 50% and lower, the oxygen permeability of silicone hydrogels surpasses that of non-silicone hydrogels. However, the increase in silicone content is associated with a decrease in the EWC. Because wettability of the material plays a crucial role in contact lens comfort, the contact lens material must include a balance of the hydrophilic monomer and the hydrophobic silicone monomer. With the increase in oxygen permeability, commercially available silicone hydrogel contact lenses can now be continuously worn for up to 30 days. The ability to wear silicone hydrogel lenses for an extended duration makes them attractive candidate materials for the delivery of therapeutic agents that must be administered for a prolonged period. Drug loading specifically in the silicone domain of the silicone hydrogel matrix is of interest as this might result in a prolonged release of the drug due to limited access to water channels in the hydrophobic silicone domain.

2.4 Methods of loading hydrophobic drugs into hydrogels

2.4.1 Soaking contact lenses in drug solution

One of the most common methods of preparing drug eluting contact lenses is by simply soaking preformed lenses in a solution containing the drug of interest. With this method, drug diffuses from the solution into the gel matrix. The lens may be soaked in an aqueous solution of drug, although with more hydrophobic drugs, increased drug loading can be achieved by placing the lens in more appropriate loading solution using an alternative solvent. Upon placement into drug releaseate, such as phosphate buffered saline (PBS) or tear solution, drug release will be slow due to reduced solubility in this media compared to the loading media in which the drug had higher solubility.

The rate of drug release from the hydrogel is governed by the laws of diffusion (Alvarez-Lorenzo, 2006). The thickness of the contact lens, the degree of lens hydration, and the drug concentration in the lens contribute to the rate of drug release. Under sink conditions, Fick's second law of diffusion may be used to predict drug release from a lens (Gulsen and Chauhan, 2005).

$$\frac{\partial C}{\partial t} = D\ \frac{\partial^2 C}{\partial y^2}$$ **(1.1)**

C is the drug concentration in the lens, *D* is the coefficient of drug diffusion and the following are the initial and boundary conditions assuming a slab-like geometry.

$$C(t = 0, y) = C_0$$ **(1.2)**

$$\frac{\partial C}{\partial t}(t, y = 0) = 0$$ **(1.3)**

$$C(t, y = h) = 0$$ **(1.4)**

C_0 is the initial drug concentration in the gel, h is the half thickness of the gel. Symmetry is assumed for the first boundary condition (**1.3**), and the second boundary condition (**1.4**) assumes equilibrium between the drug concentration in the gel at the boundaries and the surrounding release medium which is almost zero due to the relatively larger volume of the release medium and also assumes no partitioning. The following equation (**1.5**) may be used to approximate the early time release rate from a hydrophilic lens when the fractional drug release is $0 < M/M_\infty < 0.6$.

$$\frac{dM}{dt} = 2M_\infty\sqrt{\frac{D}{\pi L^2 t}}$$ **(1.5)**

M_∞ is the total amount of drug released, *D* is the coefficient of drug diffusion, and *L* is the lens thickness. It has been shown that diffusion time of a given drug from the lens matrix decreases with an increase in water content. Using silicone

hydrogel and pHEMA-containing materials, Karlgard and coworkers (2003a) also demonstrated the influence of drug and lens material properties on drug release.

Karlgard et al. (2003a) were the first to demonstrate uptake and release of various types of drugs from commercially available silicone hydrogel contact lenses. In their study, the loading and release solution was Unisol4, an unpreserved borate buffered saline, and commercial conventional HEMA-containing and silicone hydrogels were investigated. Of the model drugs tested in their study, ketotifen fumarate, a relatively hydrophobic drug showed maximal drug uptake within five hours. The relatively hydrophilic cromolyn sodium, ketorolac tromethamine and dexamethasone 21-phosphate disodium salt on the other hand showed maximal uptake within one hour. The authors also noted that the low ketotifen fumarate concentration in the loading solution may have contributed to a slow mass transfer rate to the lens surface with this drug. The effect of the drug loading solution concentration on uptake was demonstrated in a paper published later by the same group in which a higher dexamethasone phosphate loading solution concentration was used (Boone et al., 2009). For instance, comparing the uptake data from the two studies, nonionic lotrafilcon A commercial silicone hydrogel lenses soaked in 1 mg/mL dexamethasone phosphate for 4-24 h showed an uptake of 102 ± 11 μg/lens compared with an uptake of 48 ± 25 μg/lens for the same lens material soaked in 0.845 mg/mL dexamethasone phosphate for up to 50 h. Importantly, a higher drug loading concentration does not necessarily lead to greater uptake however, as uptake is

also dependent on the material properties of the lens as well as the properties of the drug. For example, ionic balafilcon silicone hydrogel lenses had similar uptake with the two loading solution concentrations used in the two studies. The drug's solubility in the loading media, the drug loading solution concentration, and the drug and material properties thus play a crucial role in contact lens drug loading and places a limitation on the maximum amount of drug that may be loaded in and subsequently released from the lens material. Fractional release of drugs indicated irreversible drug binding to the lens materials. If a substantial amount of drug remains bound to the lens matrix, the amount of drug available for absorption through the cornea is reduced thus decreasing the effectiveness of this drug delivery vehicle.

Karlgard et al. (2003b) demonstrated partial irreversible drug binding of fluorescently labeled ciprofloxacin hydrochloride in a commercial silicone hydrogel that was loaded by soaking the lenses in a ciprofloxacin/Unisol4 solution. After a 24h period of drug release, photo bleaching in an area of the lens was performed by focusing the laser beam in the area for a few minutes. The lack of fluorescence recovery in the area indicated that the ciprofloxacin was bound irreversibly to the lens matrix and that adsorption and desorption were not occurring to result in fluorescence recovery.

The hydrogel monomers from which the contact lens is made up have a strong influence on both drug loading and release. Lens composition affects

such properties such as swellability and ionic interactions with the drug which plays roles in controlling the drug uptake and release behaviour (Karlgard et al. 2003). Release of a variety of molecules from conventional polyhydroxyethyl methacrylate (pHEMA) and silicone-containing lenses, prepared via soaking, have been described extensively in the literature (Li and Chauhan, 2006; Soluri et al., 2012; Chauhan et al., 2008; Kim and Chauhan, 2008). Release profiles observed upon drug loading by the soaking method generally appear as a burst followed by a period of declining, sub-therapeutic levels of release. Also the total amount of drug loading is limited by the solubility of the drug in the loading solution as well as on the swellability of the contact lens material (Alvarez-Lorenzo, 2006). Drug loading conditions that are similar to those of drug release consequently result in similar uptake and release kinetics (Karlgard et al., 2003a). This poses a limitation on the control over drug release thus necessitating alternative drug loading strategies.

Chauhan and coworkers have synthesized model silicone hydrogels which allow for extended release. They demonstrated how release of dexamethasone, for instance, can be achieved over a period of 20 days to three months depending on the compositions of the gels (Kim et al., 2008). To demonstrate the influence of the components of the gel formulation on the release of timolol, a gel composed of the macromer used to improve solubility between the hydrogel and silicone monomers, and a gel composed of the hydrophilic monomer were prepared. Release from the material containing the hydrophilic monomer

occurred rapidly over less than two hours compared to release from the silicone macromer containing gel which lasted over five months. The amount of drug released from the macromer containing gel however, was less than that from the hydrophilic monomer. These differences in release were attributed to the differences in hydration between the two materials. Therefore, by increasing the hydrophilic monomer content in the silicone hydrogel, a shorter release duration was observed. The macromer gel was shown for illustrative purposes and would not be suitable for contact lens wear without the crucial properties provided by the hydrophilic and silicone monomers. The two gel formulations with a combination of the hydrophilic monomer, the silicone monomer, and the macromer that was more appropriate for extended contact lens wear resulted in a release duration of between 10 and 15 days. Release of the relatively more hydrophobic drug, dexamethasone, from these silicone hydrogel materials was also performed. Although the duration of release was longer with dexamethasone than with timolol, the amount released was lower due to a larger partition coefficient of dexamethasone in the silicone hydrogel.

2.4.2 Direct entrapment

Another method of loading a hydrophobic drug into the hydrogel lens matrix is by direct entrapment. This method involves addition of the drug directly to the gel formulation prior to curing. In one study, Kim and Chauhan showed release over approximately 10 h upon loading dexamethasone into pHEMA gels using this method (Kim and Chauhan, 2008). The release data indicated that not

all of the drug initially loaded was released suggesting that some of the drug remains trapped in the hydrogel matrix with this method. Also, drug loading by the direct entrapment method might lead to a loss of drug activity during polymerization.

Korogiannaki (2013) prepared a model drug-loaded silicone hydrogel by the direct entrapment method, and showed extended release of ketotifen fumarate over a period of more than two weeks. Irreversible drug binding within the hydrogel matrix was reported, with gels containing wetting agents showing a greater amount of ketotifen fumarate release compared to control gels that did not contain a wetting agent. The presence of wetting agents presumably reduced the affinity of the drug for the hydrogel matrix or allowed for the creation of diffusion channels thereby allowing more of the drug to be released.

Rather than adding the drug directly into the hydrogel formulation, a drug-eluting contact lens was developed by Ciolino et al. (2009) which involved preparation of a dispersion of fluorescein or ciprofloxacin in a polylactic-co-glycolic acid (PLGA) film. This drug or fluorescein-PLGA film was then coated with pHEMA by ultraviolet polymerization. Controlled, zero-order release for a prolonged period over four weeks was demonstrated and the release rate was tunable by adjusting the PLGA molecular mass, and fluorescein to PLGA ratio. Both PLGA and pHEMA influenced the release rate, as release from PLGA or

pHEMA alone was faster. This device would, however need to be optimized for such properties as transparency and oxygen permeability.

2.4.3 Cyclodextrins and surface functionalization with liposomes

Surface functionalization of contact lens materials with liposomes that encapsulate the hydrophobic drug is another method that has been investigated for hydrophobic drug loading into contact lens materials. Liposomes are vesicles consisting of phospholipids which, in an aqueous environment, spontaneously self-associate into concentric bilayers creating an aqueous core with a lipophilic annulus (Malam et al., 2009). Liposomes may thus be loaded with hydrophobic or hydrophilic molecules. A commercial contact lens material was surface functionalized and levofloxacin-containing liposomes were immobilized onto the lenses via surface functional groups. Prolonged release via first order kinetics was shown with this system (Danion et al., 2007).

Cyclodextrins are cyclic oligosaccharides made up of six (α), seven (β), eight (γ) or more glucopyranose rings (Del Valle, 2004). They have a hydrophilic exterior and a hydrophobic interior. They are attractive for hydrophobic drug delivery as the interior cavity forms inclusion complexes with hydrophobic molecules, thus increasing the aqueous solubility of hydrophobic drugs. β-cyclodextrins were grafted onto a pHEMA/glycidal methacrylate matrix (dos Santos, 2009). The hydrogels functionalized with pendant cyclodextrins were soaked in diclofenac sodium solution for drug loading. Drug loading was

proportional to the amount of β-cyclodextrin available on the hydrogel matrix, and hydrogels containing β-cyclodextrins had a longer duration of diclofenac release compared to gels without pendant β-cyclodextrins due to a higher affinity of the drug for the sugars.

2.4.4 Particles for controlled drug delivery

Particles encapsulating a drug have gained attention due their potential for controlling the release behaviour and release duration. Sustained release attainable by some particle systems may also assist in reducing the frequency of drug administration, and subsequently increase patient comfort and compliance. Aside from playing a role in the release kinetics, the particle may also protect the therapeutic agent from synthesis procedures (Tran, 2011). Several types of particle-based systems have been designed and investigated for drug delivery. Particle systems may be injected into tissue or intravenously, applied topically, and delivered by inhalation (Kohane, 2002). In order to provide a high local concentration of the drug over extended periods, particles may be delivered directly to the site of action, or they may be delivered systemically for a systemic effect. Furthermore, drug carriers may be delivered to the location of interest via passive or active targeting (Danhier et al., 2010).

Drug release from micro- or nanoparticles is related to the particle surface area to volume ratio, and the surface area to volume ratio is inversely related to the particle radius. The release kinetics for a monolith or reservoir drug delivery

device with a spherical geometry are defined by Fick's second law of diffusion. For a monolith particle delivery system in which the drug is uniformly dissolved or dispersed in the polymer making up the particle, the early time release rate may be approximated by equation **1.6**. For a reservoir type particle delivery system, where the drug is situated at the core of particles, the steady state release rate is approximated by equation **1.7**.

$$\frac{dM/M_\infty}{dt} = 3\sqrt{\frac{D}{r^2\pi t}} - \frac{3D}{r^2} \quad \textbf{(1.6)}$$

$$\frac{dM}{dt} = 4\pi DK(c_{reservoir} - c_{surroundings})\frac{r_0 r_1}{r_0 - r_1} \quad \textbf{(1.7)}$$

Where *M* is the mass of drug released at time, t, M_∞ is the total amount of drug released, *D* is the coefficient of drug diffusion, r is the sphere radius for a monolith device, r_0 is the outer radius and r_1 is the drug reservoir radius for a reservoir device, $c_{surroundings}$ is the drug concentration in the surroundings and $c_{reservoir}$ is the drug concentration in the reservoir, K is the drug partition coefficient.

Interestingly, it was also shown that particle size can influence the drug distribution within the particle. For instance, particles 10-20 μm in size showed a homogeneous distribution of a model hydrophilic and hydrophobic drug, however for particles larger than 40 μm, the hydrophilic drugs were distributed near the surface of the particle while the hydrophobic drug partitioned to the core of the microsphere (Berkland et al., 2003; Berkland et al., 2004).

In addition to the reasons mentioned above, particle systems also allow for the incorporation of hydrophobic drugs into a hydrophilic drug delivery system. For instance, in one study, researchers loaded a lipophilic drug into polylactic co-glycolic acid (PLGA) particles. The drug-loaded particles were then incorporated into a polyvinyl alcohol (PVA) hydrophilic hydrogel matrix. The potential for controlling drug delivery via particles was demonstrated when researchers compared the release of the drug entrapped in PLGA particles with the release of the drug from drug-loaded PLGA particles embedded in a polyvinyl alcohol (PVA) hydrophilic hydrogel matrix (Cascone et al., 2002). The delivery rates were comparable suggesting the role of particles in controlling drug delivery.

2.4.4.1 Silica particles for controlled drug delivery

Silica particles offer several advantages as drug delivery vehicles. By combining sol-gel chemistry with the emulsion process, they may be prepared at ambient temperature, and drug release may be controlled by synthesis parameters (Barbé et al., 2008). Furthermore, the compatibility of silica with biological systems has been shown (Pope et al., 1997; Carturan et al., 2001; Boninsegna et al., 2003).

The sol-gel process involves hydrolysis and condensation of silica precursors (Barbé et al., 2004). Organic or bioactive molecules may be added during formation of the oxide backbone to encapsulate the molecules within the

growing oxide matrix. The reaction kinetics, particularly the rates of hydrolysis and condensation may be tailored to control density, pore size, and structure. The choice of catalyst, the polymerization pH, and the use of various alkoxysilanes can affect the structure of the gel to control the release rate of biological agents or drugs (Ahola et al., 2001; Kortesuo et al., 2001a; Kortesuo et al., 2001b).

Silica microspheres may be produced via a water-in-oil emulsion, where water droplets containing the silica precursors and the hydrophilic drug behave like microreactors in which the sol-to-gel transition takes place (Barbé, 2008). Droplet size, and subsequently particle size is controlled by the type and amount of surfactant and solvent used, and the presence of a cosurfactant. The sol-gel chemistry that controls the internal structure of the particles then controls the drug release rate. The ability to tune the porosity of silica and subsequently drug release based on reaction conditions is therefore attractive for the preparation of materials with tunable drug release properties. With the aim to achieve higher hydrophobic drug loading, the drug may be dissolved in an oil, and an oil-in-water emulsion may be prepared to synthesize particles with the hydrophobic drug in the oily core surrounded by a silica shell.

2.4.4.2 Miniemulsion polymerization for silica particle synthesis

Due to its utility for the synthesis of a wide variety of polymer particles, as well as the ability to tune particle size, miniemulsion polymerization is an

attractive method for particle synthesis. Miniemulsion polymerization may be used to create particles with a size range approximately 50-500 nm. Using this technique, a variety of polymeric nanoparticles including those requiring radical, anionic, cationic, polyaddition, as well as polycondensation reactions involved in polysiloxane/silicate synthesis can be synthesized. As reviewed by Landfester and Mailänder (2013), it may be used to encapsulate both hydrophilic and hydrophobic agents (Paiphansiri et al, 2006; Lorenz et al., 2008). The process of miniemulsion polymerization involves the dispersion of stable droplets in a continuous phase. An ultrasonicator or homogenizer is used to apply high shear to a macroemulsion consisting of a broad droplet size distribution in order to create small droplets with a narrow size distribution. In an oil-in-water emulsion, the water is the larger continuous phase, whereas in a water-in-oil emulsion, the oil phase is the continuous phase. An oil-in-water system is utilized to encapsulate hydrophobic molecules, whereas water-in-oil emulsions are used to prepare particles encapsulating hydrophilic agents. As hydrophobic drug delivery is the focus of this research, the oil-in-water miniemulsion system is described here.

An oil-in-water miniemulsion consists of oil, water, and a surfactant. The surfactant molecules sit at the oil-water interface and stabilize oil droplets by lowering the surface tension. Both the type and amount of surfactant play a major role in controlling the size of the miniemulsion droplets and subsequently the particle diameter. Several miniemulsion polymerization recipes also include

a hydrophobe, which acts as a costabilizer molecule in the oil droplet, specifically acting as an osmotic pressure agent and counterbalancing the Laplace pressure. PVA particles containing the antibiotic erythromycin estolate were prepared using miniemulsion polymerization, and release over 300 h that occurred presumably with polymer degradation was shown with this polymer particle system (Park and Kim, 2005).

Landfester et al. (2000) demonstrated that polyaddition reactions may also be conducted with the miniemulsion technique to create polymer particles with a size ranging between 30 nm and 600 nm. The dependence of particle diameter on the chemical nature of the monomers, the type and quantity of surfactant, and the pH of the reaction mixture was shown. More recently, Pang et al. (2010) described a procedure for synthesizing nano-sized particles with an oil core and a silica shell using a miniemulsion polymerization technique. Polydimethylsiloxane (500 cSt) oil and tetraethoxysilane (TEOS) and octadecyltrimethoxysilane (OTMS) silica shell precursors were mixed with an aqueous phase consisting of the anionic surfactant sodium lauryl sulphonate (SLS) and the non-ionic surfactant TritonX-100 (T100). Sonication was used to create nanometer-sized droplets, and the pH was raised to 7.5 to allow for the hydrolysis and condensation reactions between TEOS and OTMS that form the silica shell. The reaction schemes for the hydrolysis and condensation reactions are shown in **Figure 2.4**. The authors showed release of the internal silicone oil from these particles demonstrating their potential use in hydrophobic coatings.

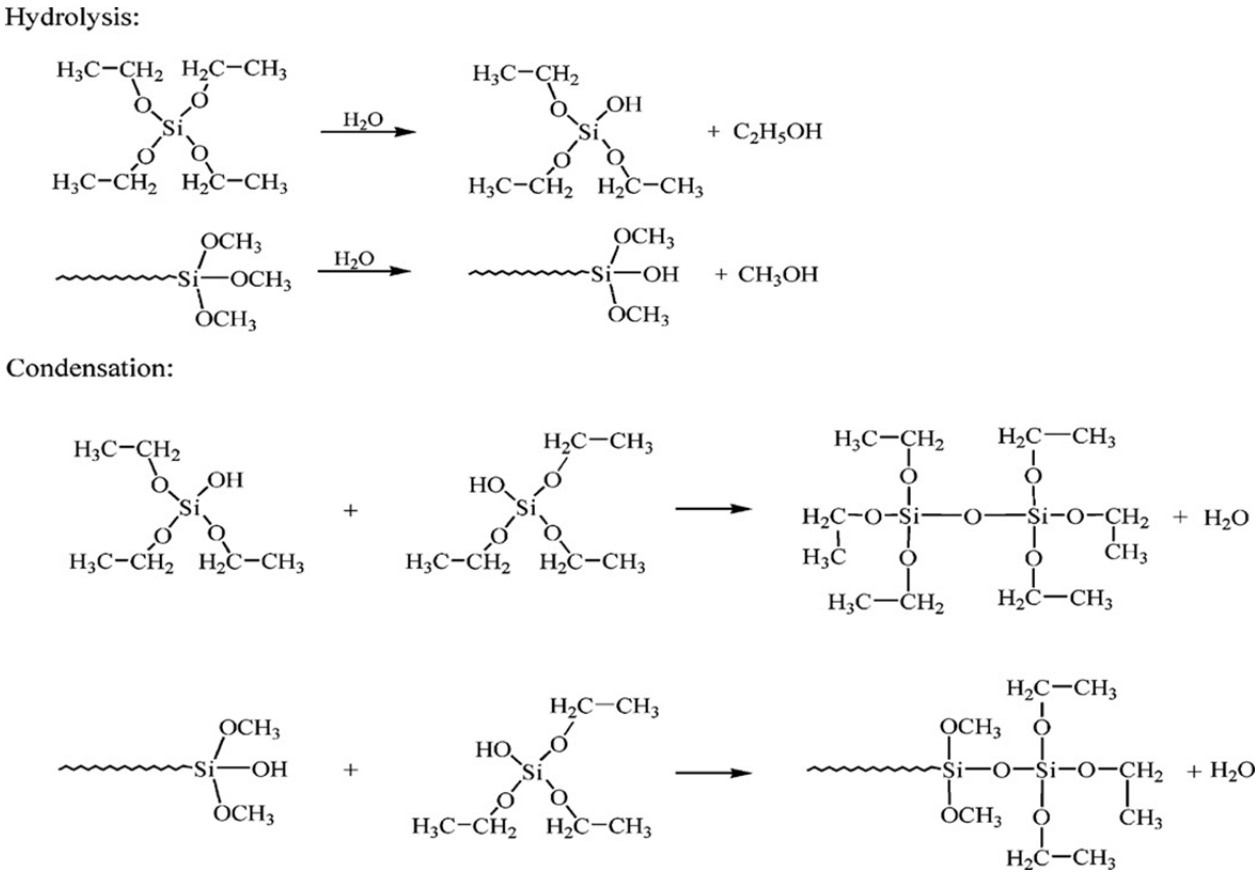

Figure 2.4. Hydrolysis and condensation reactions between TEOS and OTMS. Reprinted with permission from Pang, H., S. Zhou, L. Wu, M. Chen and G. Gu, "Fabrication of silicone oil microcapsules with silica shell by miniemulsion method," Colloids and Surfaces A: Physiochemical and Engineering Aspects. 364, 42-48 (2010). Copyright 2010. Elsevier.

2.4.4.3 Microemulsion polymerization for silica particle synthesis

The microemulsion technique also has the potential to generate particles within an appropriate size range. Lawrence and Rees (2012) describe applications of microemulsions for parenteral, pulmonary, and topical delivery. Vandamme (2002) describes the preparation of microemulsions and their

application for ophthalmic drug delivery. Microemulsions are thermodynamically stable isotropic systems that do not require the input of significant energy for their formation. They consist of an aqueous phase, an oil phase, a surfactant and sometimes a co-surfactant. As with a miniemulsion, the oil phase makes up the internal phase of nanodroplets of an oil-in-water system. These droplets are stabilized by a surfactant film at the interface between the aqueous and oil phases. The surfactant content in a microemulsion is substantially higher than that in the miniemulsion at a weight content of approximately 10%. This high surfactant concentration is required to stabilize the large oil/water interfacial area created with the formation of nanodroplets. Oil in water microemulsions consist of a low oil content (1-10%). Due to a high level of dispersion of the internal phase and a droplet size in the range of 10-100 nm, microemulsions are transparent in appearance.

To prepare particle-loaded HEMA hydrogels, Gulsen and Chauhan (2004) used a microemulsion method to form nanosize droplets. The addition of OTMS was used to form a silica shell around particles presumably to prevent the destabilization of particles upon addition of the microemulsion into the gel formulation. Transparent gels were obtained and lidocaine release over eight days was demonstrated. In addition to using OTMS as a silica shell precursor Pang et al. also included TEOS to create silica microparticles with an oil core for slow release of silicone oil from the particles (Pang et al, 2010). In another study Underhill and coworkers described the synthesis of oil-filled silica nanocapsules

for lipophilic drug uptake using OTMS and tetramethoxysiloxane (TMOS) for formation of the silica shell (Underhill et al, 2002). TMOS provides additional reactive groups to allow for extension of the silica network away from the head groups of OTMS. With the polycondensation reactions, a three dimensional cross-linked polysiloxane/silicate network is formed that results in a film that is more stable than the layer formed by crosslinking OTMS alone. **Figure 2.5** is a schematic of the silica shell formed with OTMS and TMOS as shell precursors.

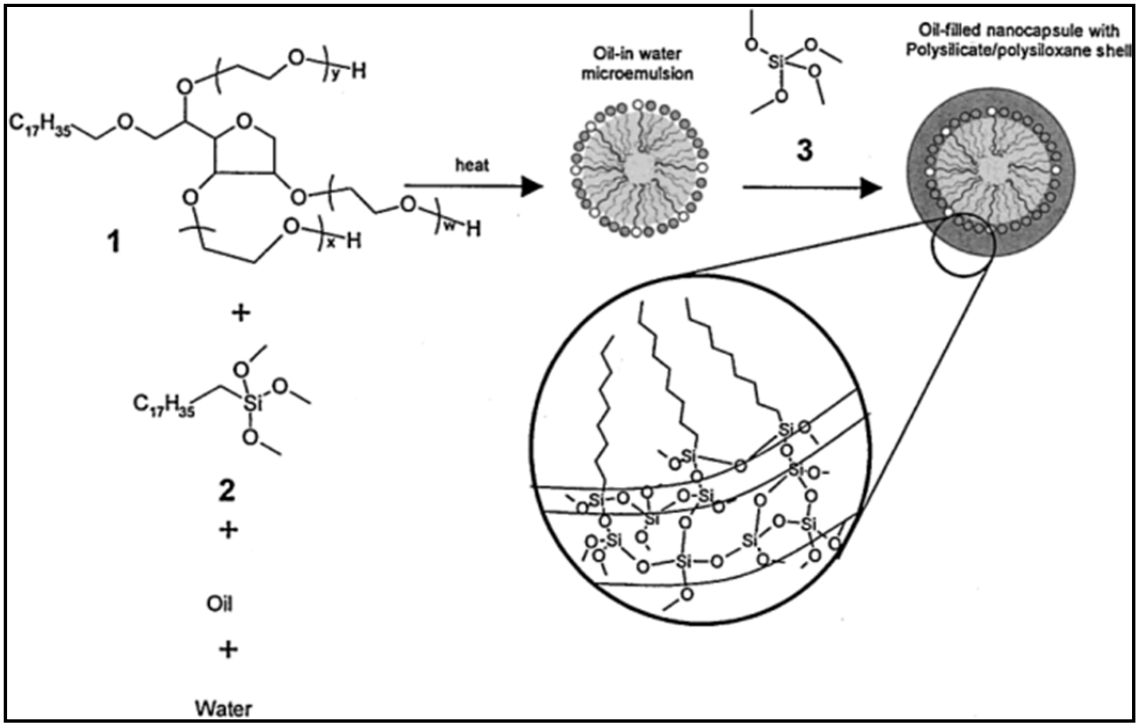

Figure 2.5. Schematic of oil-filled silica nanocapsule formation with OTMS and TMOS as silica shell precursors. (1) Brij 97 surfactant, (2) OTMS, (3) TMOS. Figure from Underhill et al., 2002. Reprinted with permission from Underhill, R.S, A.V. Jovanovic, S.R. Carino, M. Varshney, D.O. Shah, D.M. Dennis, T.E. Morey, R.S., Duran, "Oil-filled silica nanocapsules for lipophilic drug uptake: implications for drug detoxification therapy," Chem. Mater., 14, 4919-4925 (2002). Copyright 2002 American Chemical Society.

2.4.4.4 Embedding drug-containing particles in a hydrogel matrix

Gulsen and Chauhan have described the incorporation of lidocaine-loaded silica nanoparticles into a pHEMA hydrogel and showed prolonged release of lidocaine (Gulsen and Chauhan, 2004). The aim of loading the drug within particles and then embedding drug-loaded particles into the gel matrix is to provide an additional barrier to drug transport. The duration of drug release is

presumably prolonged since the entrapped drug molecules would need to diffuse out of the particle and then out of the gel matrix. This research group has also demonstrated the incorporation of lidocaine and cyclosporine A in alternative colloidal delivery vehicles dimyristoyl phosphatidylcholine liposomes and Brij surfactant micelles respectively for incorporation into and prolonged release from pHEMA-based hydrogels (Gulsen et al., 2005; Kapoor et al., 2009).

Lu et al. (2012), prepared core cross-linked polymer micelles containing a hydrophobic model drug, 7-hydroxy-9H-(1,3-dichloro-9,9'-dimethylacridin-2-one), for the preparation of pHEMA gels embedded with these particles. By inclusion of an acryloyl group in the hydrophobic segment of the polymer diblock that made up micelles, free radical polymerization of the acryloyl groups allowed for the formation of core cross-linked micelles that were stable in the presence of HEMA monomer. Furthermore, an allyl group at the terminus of the hydrophilic segment of the polymer diblock allowed for micelles to be chemically bound within the hydrogel matrix. Release of the model drug was faster in control pHEMA gels containing no micelles compared with gels containing the model drug encapsulated in micelles. A HEMA-based hydrogel embedded with silica shell cross-linked amphiphilic block copolymer micelles was also prepared (Lu et al., 2013). The hydrophobic block of the copolymer forms the core of the micelles and contains the hydrophobic dexamethasone acetate drug. The presence of drug-loaded silica shell cross-linked micelles within the hydrogel resulted in extended delivery of the drug for 30 days, and drug diffusion from the

micelles rather than diffusion from the hydrogel matrix was determined to be the rate-limiting step for release with this material.

The previous studies described the incorporation of aqueous particle suspensions within a HEMA-based hydrogel matrix. Being hydrophilic, the HEMA monomer allows for the incorporation of water within the gel matrix without a subsequent loss of transparency in the material. pHEMA is however, not suitable for extended lens wear. As mentioned previously, silicone-containing contact lenses can be worn for up to 30 days due to increased oxygen permeability (Tighe, 2004). Therefore, the ability to embed particles into a silicone hydrogel matrix is quite desirable. In a study by the Chauhan group, Jung et al. prepared silicone hydrogels embedded with timolol-loaded nanoparticles and showed release of this glaucoma drug at room temperature over a one-month period (Jung et al., 2013). In this system, propoxylated glyceryl triacrylate (PGT) particles loaded with the hydrophobic form of timolol were added to a model silicone hydrogel formulation prior to curing under ultraviolet light or by soaking a commercial silicone hydrogel lens in a solution of timolol-PGT particles in ethanol. Adding drug-loaded particles to the silicone hydrogel formulation prior to curing resulted in timolol release over one month at room temperature compared with the soaking method that released timolol over a two week period. Release of timolol from the nanoparticles, as opposed to diffusion of the drug from the lens matrix is believed to be the rate limiting step for drug release. Furthermore it is the hydrolysis of the speculated ester bonds

between timolol and the cross-linked PGT network that is believed to control the rate of release from particles (Jung and Chauhan, 2012).

The incorporation of drug-containing particles in the gel formulation prior to curing is a promising method of drug loading for achieving prolonged release. If release from particles is the rate-limiting step, there exists the potential to tune particle properties to control the release behavior of the drug of interest from the hydrogel.

2.5 Objectives of current research

The use of drug-loaded particles embedded in a hydrogel matrix as a material to control drug delivery is attractive due to the increased control over drug loading, and to the additional barrier to drug transport provided by the presence of particles. The increased oxygen permeability and comfort achievable with the incorporation of siloxy groups in the hydrogels, and therefore its growing popularity among contact lens wearers makes this material an important one for incorporation of drug-loaded particles. The inclusion of a hydrophobic silicone-containing monomer, such as a methacryloxypropylTris (tri-methylsiloxylsilane) (TRIS), in the gel formulation however results in phase separation upon addition of the aqueous particle suspension. The current work aims to incorporate an aqueous suspension of drug-loaded silica particles into a silicone hydrogel formulation while reducing phase separation to obtain a silicone

hydrogel material with embedded drug-loaded silica particles for controlled drug delivery of a hydrophobic drug. It is hypothesized that:

- Use of a hydroxylated silicone monomer will allow for a homongeneous gel formulation containing the hydrophilic and hydrophobic monomers, and the aqueous drug-containing particle suspension
- Incorporation of drug-containing particles with a silica shell will result in localization of the particles in the silicone domains of the hydrogel matrix
- The use of methacryloxypropyltriethoxysilane (MATO), an alternate silica shell precursor, compared to TEOS will result in slower release of the drug since the silica particles made of the polymerizable MATO when initially added to the gel formulation will associate with the silicone domain, remain immobilized in the silicone domain due to the methacrylate group present in this shell precursor, and therefore release drug at a slower rate due to reduced access to water channels in the gel matrix

Two methods are described for the synthesis of drug-loaded silica particles namely miniemulsion polymerization and microemulsion polymerization. Drug release studies are done to demonstrate the release profile of a model hydrophobic drug, dexamethasone, from a model silicone hydrogel material containing embedded drug-loaded particles. Specific objectives are as follows:

- Synthesis of drug-containing silica particles with tunable diameters
- Improvement of stability of drug-containing silica particles in PBS
- Preparation of a model silicone hydrogel material with embedded drug-containing particles that can release drug in a concentration-dependent manner over a prolonged period
- Characterization of silicone hydrogel materials embedded with drug-containing particles by transmission electron microscopy (TEM)

3. MATERIALS AND METHODS

3.1 Reagents

The model drugs atropine, acetazolamide, and dexamethasone were purchased from Sigma-Aldrich (Oakville, ON). All other reagents and their sources are listed in **Appendix A**.

Model drugs used in this work are described below. The hydrophobicity of a solute is related to its logP value. A higher positive value indicates a more hydrophobic drug, while a negative logP value is indicative of a hydrophilic drug.

Acetazolamide

Acetazolamide is carbonic anhydrase inhibitor used to treat glaucoma. Another indication includes the treatment of symptoms of altitude sickness. In conjunction with other medications it is also used to reduce edema and for controlling seizures in certain types of epilepsy (MedlinePlus, 2010). The structure of acetazolamide is shown in **Figure 3.1** and its logP value is listed in **Table 3.1**.

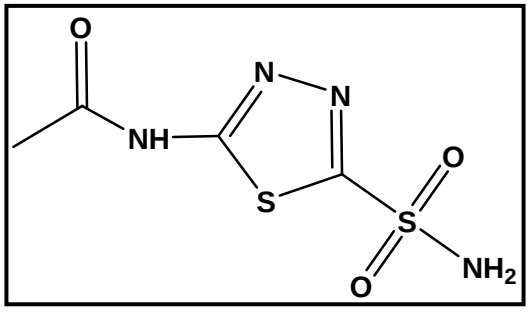

Figure 3.1. Chemical structure of acetazolamide.

Atropine

Atropine is nonselective muscarinic antagonist used to dilate pupils prior to an eye examination. It is also indicated for the relief of pain due to swelling and inflammation of the eye (MedlinePlus, 2011). Additionally, based on clinical studies conducted with children aged 6-13 years old, topical atropine has been reported to slow the progression of myopia (Shih et al., 2001; Chua et al., 2006; Tong et al, 2009). The structure of atropine is shown in **Figure 3.2** and its logP value is listed in **Table 3.1**.

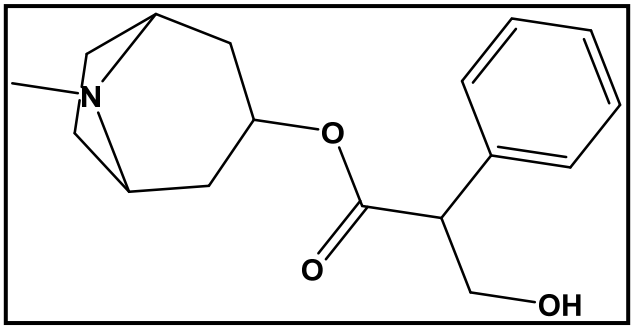

Figure 3.2. Chemical structure of atropine.

Dexamethasone

Dexamethasone is a corticosteroid prescribed to relieve inflammation, certain types of arthritis, severe allergies, asthma, and certain types of cancer. In the eye, dexamethasone is used to reduce irritation, redness, burning, and swelling in the eye, and sometimes after surgery (Medline Plus, 2010). The structure of dexamethasone is shown **Figure 3.3** and its logP value is listed in **Table 3.1**.

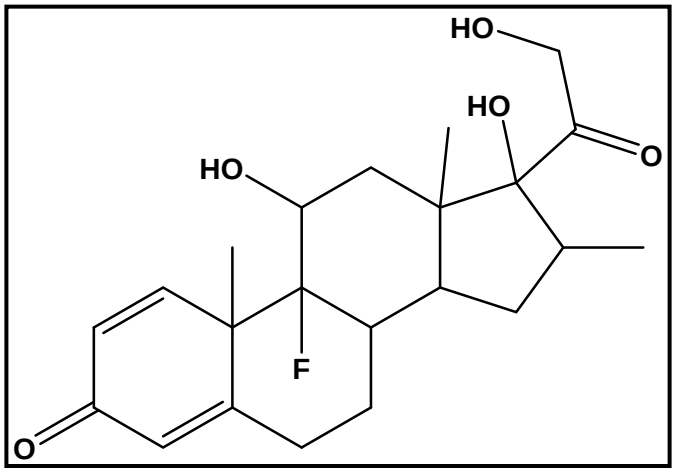

Figure 3.3. Chemical structure of dexamethasone.

Table 3.1. Model drugs and their logP values.

Drug	LogP
Acetazolamide	-0.26[a]
Atropine	1.83[b]
Dexamethasone	1.83[c]

(a) Remko and von der Lieth, 2004 (b) Moriguchi et al., 1994 (c) Yakushiji et al., 1999.

3.2 Miniemulsion for drug-containing silica particle synthesis

Drug-loaded silica particles were synthesized as described by Pang et al. (2010). Both atropine and acetazolamide were evaluated as model drugs using this method. Detection of the drugs was by UV spectrophotometry. Unless otherwise indicated, drug loaded silica particles were prepared as follows. An aqueous phase consisting of 10 mL deionized water, 0.025 g of the anionic surfactant sodium dodecyl sulphate (SDS) and 0.075 g of the non-ionic

surfactant TritonX-100 was prepared. An oil phase was prepared consisting 1 g polydimethylsiloxane (PDMS, 500 cSt), 92 mole%, 1 g tetraethyl orthosilicate (TEOS), 8 mole% (0.15 g) octadecyltrimethoxysilane (OTMS), and 0.16 wt/wt% (0.02 g) (wt drug/wt particle suspension) atropine or acetazolamide. The two phases were mixed on ice, and then the mixture was sonicated in an ice bath at 100% intensity for 15 s using a Q-Sonica S-4000 sonicator equipped with a 1.27 cm (1/2") sonication probe to create nanometer-sized droplets. The pH of the solution was raised to 7.5 using sodium hydroxide (NaOH), and the solution was stirred for 24 h to allow for formation of the silica shell. A schematic representation of particle synthesis using the miniemulsion polymerization technique is shown in **Figure 3.4**.

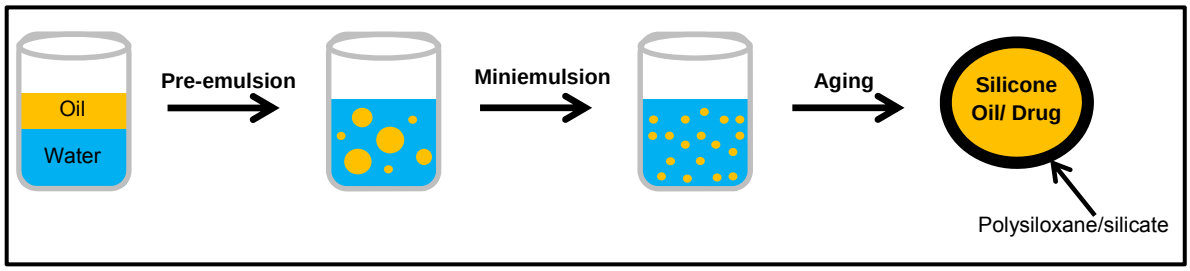

Figure 3.4. Synthesis of silica particles by miniemulsion polymerization technique. Figure adapted from Pang et al. (2010).

3.2.1 Particle characterization by dynamic light scattering (DLS)

Particle size was determined by DLS. A HeNe laser with a 633 nm light source was used and detection was at a 90° angle using a Brookhaven Instruments Corporation detector. Particle samples were diluted, and the magnification and filter were adjusted such that the average count rate was between 100 and 250 kilocounts per second. Repeated measurements of each sample were performed, and the reported values are the mean effective particle diameter ± standard deviation (SD). Sonication intensity and duration were varied to determine the sonication settings required to minimize drug-containing particle size.

3.2.2 Particle stability in PBS

Three methods were investigated for the purpose of improving particle colloidal stability in PBS in order to optimize the ability to incorporate the particles into the silicone hydrogel materials. Particles were prepared at various aging step pH values. Copolymer adsorption onto particles was assessed to improve particle stability via steric stabilization. Particles were prepared using various ratios of surfactants. Stability of the systems in PBS was assessed visually.

3.2.2.1 Preparation of particles at various aging step pH values

A stock solution of the aqueous and oil phase mixture described in section **3.2** was prepared by scaling up all reagents by a factor of ten. The stock mixture was then sonicated at 100% intensity for 10 minutes. 10 mL of the miniemulsion,

i.e. the droplet suspension, were aliquoted to each of six vials, and the pH of each miniemulsion was then adjusted to values ranging from 4.5-9.5. Particle size was measured by DLS and particle stability in PBS was examined visually.

3.2.2.2 Copolymer adsorption onto particles to improve particle stability via steric stabilization

In order to investigate the potential of polymer adsorption onto particles for improving particle stability in PBS, various concentrations of 4.4 kDa dimethylsiloxane polyethyleneoxide (DMS-PEO) copolymer were first prepared in deionized water. 750 µL of the respective polymer concentration was mixed with 250 µL of empty or atropine-containing silica particle suspensions. The samples were incubated for 30 minutes with gentle inversion of the samples at 10 minute intervals. The stability of these particles in PBS was visually examined, and polymer adsorption on the particles was measured by electrophoretic mobility measurement. Since the presence of surface charge on particles results in their interaction with an applied electric field, the charged particle will migrate toward the oppositely charged electrode. Polymer incubated samples were diluted in 5 mM NaCl and electrophoretic mobility measurements were done using a ZetaPlus zeta potential analyzer from Brookhaven Instrument Corporation with 10 runs (15 cycles per run) per sample.

3.2.2.3 Preparation of particles using various ratios of surfactants

The role of surfactant composition on particle stability in PBS was examined. Acetazolamide-containing particles were prepared as described in section **3.2**, except using various weight percentages of SDS relative to TritonX-100 surfactant. The total surfactant content remained at 1% weight by volume of water. Particle size was measured by DLS, and particle stability in PBS was visually examined.

3.2.3 Effect of acetazolamide loading on particle diameter

Acetazolamide-containing particles were prepared as described in section **3.2,** except using 20 mg, 200 mg, or 2000 mg acetazolamide to determine the effect of drug loading on particle size. Particle size was measured by DLS.

3.3 Microemulsion for dexamethasone-containing silica particle synthesis

3.3.1 Dexamethasone partitioning in oil/deionized Water

Since it is crucial that the drug to be loaded partitions into the oil phase in order to achieve high drug loading in the nanoparticle core, a partitioning study was done to determine whether dexamethasone partitions preferentially in four candidate oils or in deionized water in order to select an appropriate internal oil for microemulsions. Candidate internal phase oils were chosen based on previous use in the preparation of microemulsions for potential ophthalmic drug delivery applications (Vandamme, 2002; Li et al., 2007).

A 0.04 mg/mL solution of dexamethasone in deionized water was prepared. The concentration was selected to ensure that the amount of dexamethasone present in samples was below the water solubility limit of 0.1 mg/mL for dexamethasone (The Merck Index, 2006), and the solubility limit did not hinder dexamethasone diffusion into the aqueous phase. 1.5 g of each of isopropyl myristate, soybean oil, triacetin, or ethyl butyrate was added to vials in triplicate. 1.5 mL of the dexamethasone solution was added to each vial and the vials were stirred for four hours. The vials were then left on the bench top for approximately 21 h. The aqueous phase was then carefully aspirated from each vial using a glass pipette. Dexamethasone concentration in the aqueous phase was determined by high performance liquid chromatography (HPLC).

3.3.2 Particle synthesis by microemulsion polymerization technique

Drug-loaded silica nanoparticles were prepared similar to the protocols described by Gulsen and Chauhan, 2004 and Underhill et al., 2002, except using ethyl butyrate as the internal phase oil, dexamethasone as the model drug, and MATO in addition to OTMS as silica shell precursors. MATO was selected as a silica shell precursor as this compound, compared with TEOS, contains an acryl group which would enable chemical bond formation between the silica shell of the particles and the hydrogel matrix during polymerization of the silicone hydrogel formulation. See **Figure 3.5** for a comparison of MATO and TEOS chemical structures.

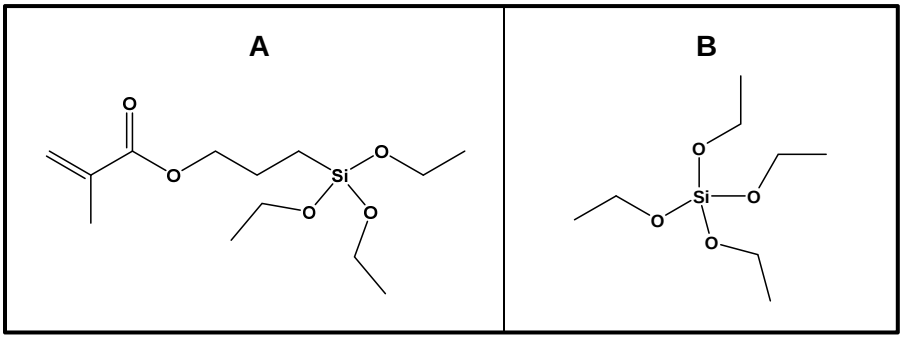

Figure 3.5 (A). MATO and **(B).** TEOS

Of the oils tested in the partitioning study, ethyl butyrate contained the highest concentration of DXM and as such was selected as the internal phase oil for the preparation of DXM-containing silica nanoparticles. Drug-containing silica nanoparticles were prepared as follows. Dexamethasone, either 0.02 g (0.17% wt/wt) or 0.01 g (0.085% wt/wt) was mixed in 0.120 g ethyl butyrate and 0.040 g OTMS (38 mole %). 10 mL of deionized water was added, followed by 1.5 g polyoxyethylene (10) oleyl ether (Brij 97) surfactant. The microemulsion was formed by stirring the solution at 800 rpm at 60°C for at least 1.5 h. The solution was then stirred at room temperature prior to the addition of 0.050 g MATO (62 mole %). Alternatively samples were prepared with 0.036 g TEOS (62 mole %), or no shell precursors. The pH was adjusted to 7.4 with 1M NaOH and the solution was stirred for 24 h to allow for the reactions between OTMS and MATO/TEOS that form the silica shell. A schematic representation of particle synthesis using the microemulsion polymerization technique is shown in **Figure 3.6.** Particle size was measured by DLS.

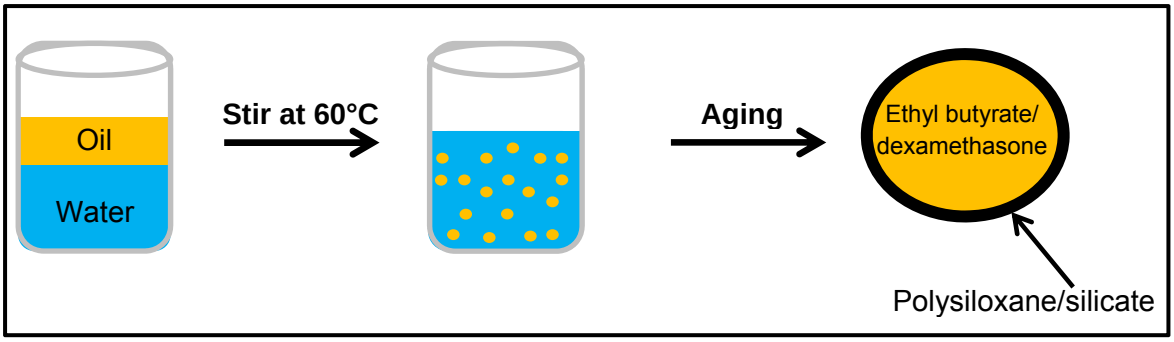

Figure 3.6. Synthesis of silica nanoparticles by microemulsion polymerization technique.

3.4 Incorporation of dexamethasone-containing silica particles in a model silicone hydrogel

3.4.1 Water tolerance of hydrophilic and silicone monomers

A water tolerance study was done to investigate the potential of a hydroxylated silicone monomer to allow the incorporation of an aqueous drug-loaded particle system in the gel formulation. Hydrophilic (*N,N*-dimethylacrylamide or 2-hydroxyethyl methacrylate) and hydrophobic silicone (3-methacryloxypropyltris(trimethylsiloxy)silane or 3-(3-methacryloxy-2-hydroxypropoxy)propylbis(trimethylsiloxy)methylsilane) monomers were purified by passing through inhibitor remover to remove monomethyl ether hydroquinone inhibitor. The monomers were then added to glass vials at a 90:10 molar ratio. Deionized water was added and the vials were stirred. Water was added until the mixture appeared to separate into phases.

3.4.2 Synthesis of HEMA/TRIS-OH silicone hydrogels containing dexamethasone-loaded particles

The monomers 2-hydroxyethyl methacrylate (HEMA) and 3-(3-methacryloxy-2-hydroxypropoxy)propylbis(trimethylsiloxy)methylsilane (TRIS-OH) were selected for gel synthesis based on the results of the water tolerance study. These monomers as well as the crosslinker ethylene glycol dimethacrylate (EGDMA) were purified by passing each through inhibitor remover pellets to remove monomethyl ether hydroquinone inhibitor. 87 mole % HEMA (2.07 g), 10 mole % TRIS-OH (0.75 g), 3 mole % EGDMA (0.108 g), the microemulsion (0.8 g), and 0.0015 g of the photoinitiator Irgacure 184 were added to a glass vial and mixed by vortexing. A 23-gauge needle was used to add the gel mixture to a mold containing a 0.5 mm Teflon spacer. The gel was cured using ultraviolet light at 365 nm for 15 min. The cured gels were dried in a 37°C oven for approximately 15-20 h.

3.4.2.1 Synthesis of HEMA/TRIS-OH, and HEMA hydrogels

A control HEMA/TRIS-OH hydrogel was prepared for equilibrium water content (EWC) and transparency studies, and HEMA, and HEMA/dH_2O hydrogels were prepared for TEM analysis. The HEMA/TRIS-OH gel was prepared as described in section **3.4.2**, except without inclusion of the particle suspension. HEMA and HEMA/dH_2O hydrogels were prepared as described in section **3.4.2**, except using 97 mole % HEMA (2.3 g) for the HEMA hydrogel, and 97 mole % HEMA (2.3 g) and 0.8 g dH_2O for the HEMA/dH_2O hydrogel.

3.4.3 Characterization of Hydrogels

3.4.3.1 Equilibrium water content

Disks with a diameter of 0.79 cm (5/16") were dried in the 37°C oven and then placed under vacuum to thoroughly dry them prior to measuring the dry mass. The disks were subsequently placed in wells of a 48-well plate. 1 mL of deionized water was added to the wells, the plate was covered with an adhesive film to reduce evaporation and left at room temperature. The mass of the disks were measured the following day and each subsequent day until there were no further changes. The EWC was calculated according to equation **(3.1)**.

$$EWC\ (\%) = \left(\frac{Mass_{wet} - Mass_{dry}}{Mass_{dry}}\right) \times\ 100 \quad \textbf{(3.1)}$$

3.4.3.2 Transparency

Disks with a diameter of 0.56 cm (7/32") were placed in individual wells of a 48-well plate and 1 mL of deionized water was added to each well. The disks were swollen for at least 48 h prior to removing from the well, dabbed on a lint-free tissue and placed into the individual wells of a 96-well plate. 200 µL of deionized water was added to each well and the plates were scanned at a wavelength range of 300 nm to 800 nm obtaining transmittance readings within the wavelength region for visible light. Wells containing deionized water only were used to blank sample wells.

3.4.3.3 Transmission electron microscopy

Thin sections (80-100 nm) of hydrogel samples were cut at room temperature with a diamond knife on a Leica UCT Ultramicrotome and picked up onto Cu grids. The sections were viewed in a JEOL JEM 1200 EX TEMSCAN TEM (JEOL, Peabody, MA, USA) operating at an accelerating voltage of 80 kV.

3.4.3.3.1 TEM for dexamethasone-containing particle suspensions

In order to investigate whether regions of darker contrast spots observed on micrographs of silicone hydrogels were silica particles, silica nanoparticle suspensions were observed by TEM. 2 µL of particle suspension was added to 10 µL water. A 3 µL droplet of this dilution was placed on a Formvar-coated grid and allowed to air-dry. Once dried, the grids were viewed in a JEOL JEM 1200 EX TEMSCAN TEM (JEOL, Peabody, MA, USA) operating at an accelerating voltage of 80 kV.

3.5 Dexamethasone release study

Gels were soaked in PBS for 1 h with gentle shaking to assist in soaking the gels in order to punch out disks for drug release, EWC, and transparency studies. Disks with a diameter of 0.79 cm were punched out using a cork borer. The disks were placed in a 37°C oven to dry. Prior to beginning the drug release studies, dry disks were weighed and then placed into 1.5 mL microtubes. 1 mL of PBS was added to the tubes, and the tubes were placed in a 34°C water bath

and shaken at 20 rpm. At selected time points, the samples were removed from the water bath, the disks were removed from the microtubes, gently dabbed with lint-free tissues and placed into new 1.5 mL microtubes. 1 mL of fresh PBS was added to the tubes and the tubes were returned to the water bath. Drug release samples were stored at 4°C until they were analyzed by HPLC. The releaseate from disks embedded with empty particles for each sample type served as a control and was also analyzed by HPLC to ensure that observed peaks were due to the presence of dexamethasone and not some other artifact.

HPLC analysis was performed using a Waters system equipped with a 2707 Autosampler, 2489 UV/Visible detector and 1525 binary HPLC pump. The column used was a reversed-phase Atlantis C18 column (100 mm x 4.6 mm). The flow rate was 1.0 mL/min using an acetonitrile:deionized water (40:60) solution as described by Mateen (2012). The retention time was 3.8 to 3.9 min at an absorbance of 254 nm.

4. RESULTS AND DISCUSSION

In order to synthesize drug-loaded silica particles for preparing silicone hydrogels embedded with drug loaded particles, the miniemulsion polymerization technique was first utilized based on a method described by Pang et al. (2010) for preparing microcapsules with a silica shell and an oil core for slow release of silicone oil from particles. By using a similar procedure and adding the hydrophobic drug to the organic phase prior to mixing with the surfactant containing aqueous phase, it was expected that silica particles with an oil core containing the hydrophobic drug would be synthesized. This method for preparing drug-containing silica particles was attractive as the use of water as the bulk phase would allow for direct incorporation into the silicone hydrogel formulation without the need for an additional processing step for removal of solvents.

4.1 Optimization of silica particle size

Various parameters were evaluated to optimize the size of the particles. The diameter of the resultant particles was measured by dynamic light scattering. As seen in **Figure 4.1,** an increase in sonication intensity resulted in a decrease in particle size as expected.

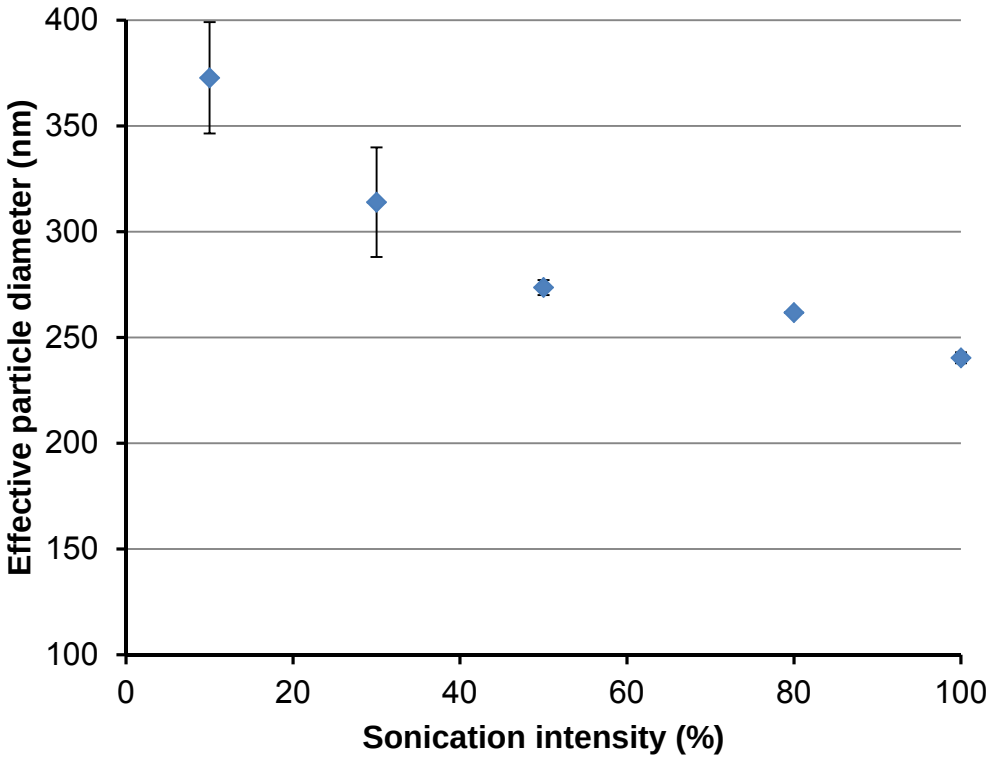

Figure 4.1. Effect of sonication intensity on particle diameter. Data are the mean effective particle diameter (± SD) for three repeat measurements.

For samples prepared at 100% intensity, it was found that increasing the time of sonication up to 15 s led to a decrease in the size of the particles, but times greater than 15 s did not lead to a significantly decreased particle size as shown in **Figure 4.2**. There was no statistical difference in particle size for samples sonicated for 15 s, 20 s and 30 s ($p>0.05$). It was therefore determined that sonication at 100% intensity for 15 s would allow for the minimum effective particle diameter for silica particles containing atropine.

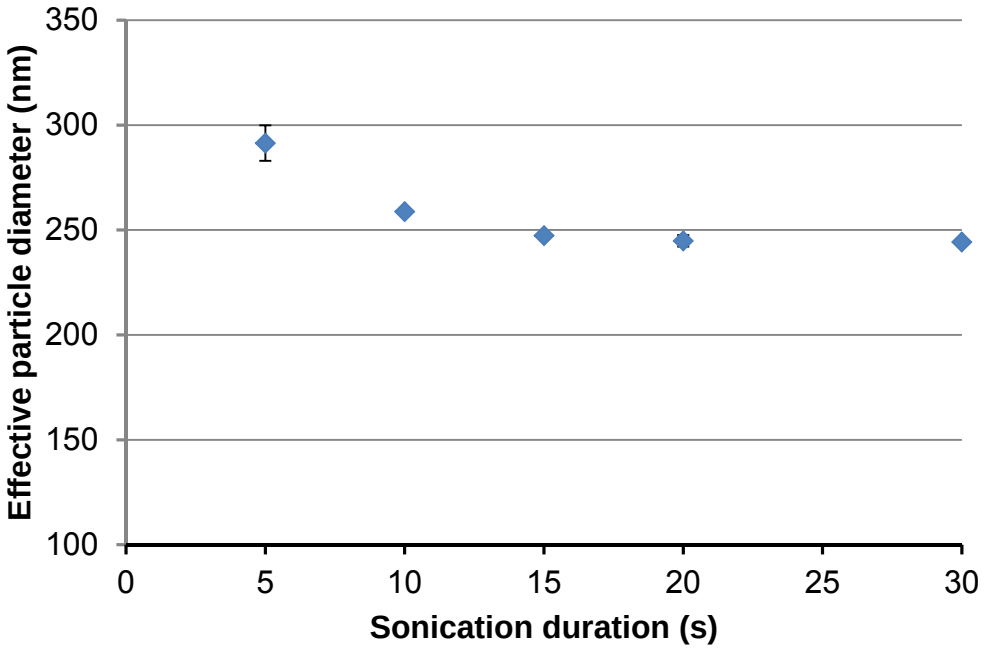

Figure 4.2. Effect of sonication duration on particle diameter. Data are the mean effective particle diameter (± SD) for three repeat measurements.

4.2 Factors affecting drug-loaded silica particle stability in PBS for particles prepared by miniemulsion technique

One of the advantages of using a drug-loaded particle system is the ability to tune particle properties to control drug release. Atropine-containing silica microparticles settled to the bottom of the vial when placed in phosphate buffered saline (PBS) at pH 7.4 suggesting that their colloidal stability and therefore the ability to incorporate into a gel formulation prepared under aqueous conditions was potentially problematic.

Pang et *al*. (2010) suggest that an aging step pH of 7.5 was optimal for obtaining good particle stability. Cihlar (1993) showed that the hydrolysis and condensation reactions of TEOS are pH dependent, with the hydrolysis rate at a

minimum at pH 7.0, and the condensation rate of the hydrolysis products at a minimum at approximately pH 2.0. Pang et al. (2010) state that, at a low pH where the rate of hydrolysis is faster than the rate of condensation, some products of hydrolysis may leave the oil/water interface where the shell is formed and enter the aqueous phase. This may cause partial gel formation and subsequently lead to particle aggregation. Since performing the aging step at a pH outside the optimal pH range for TEOS reactions may result in inefficient silica shell formation, this was thought to contribute to a lack of stability in PBS. Atropine-containing particles were synthesized at various pH values in order to investigate whether suspension of particles in PBS could be improved by changing the aging step pH. However, as shown in **Figure 4.3**, there was generally no effect of pH on the particle diameter of samples, although a decrease in the pH was shown (**Figure 4.4**) to marginally increase the particle stability in PBS.

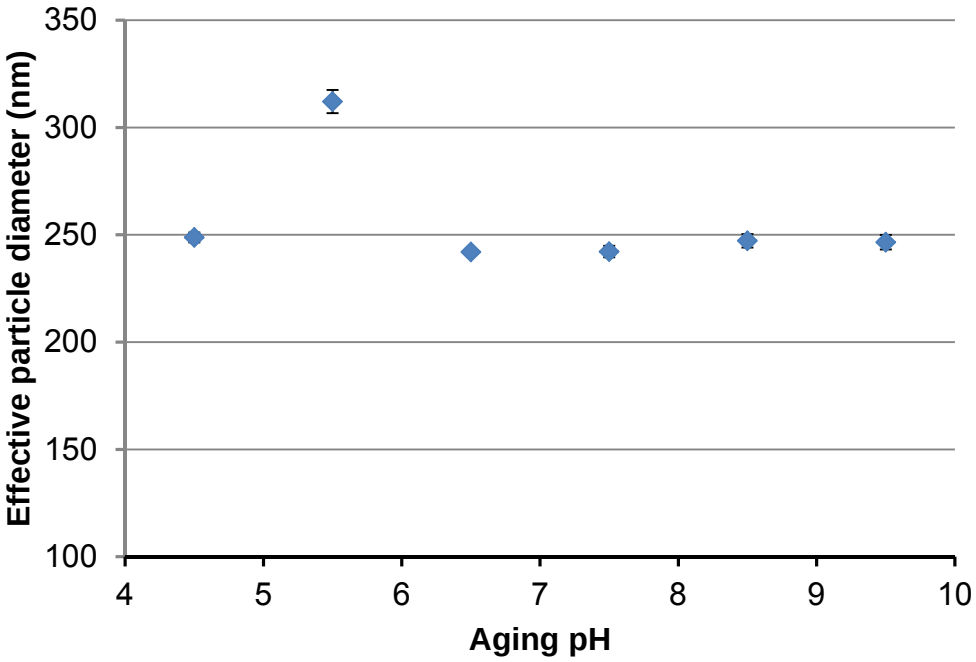

Figure 4.3. Effect of aging step pH on particle diameter. Data are the mean effective particle diameter (± SD) for three repeat measurements.

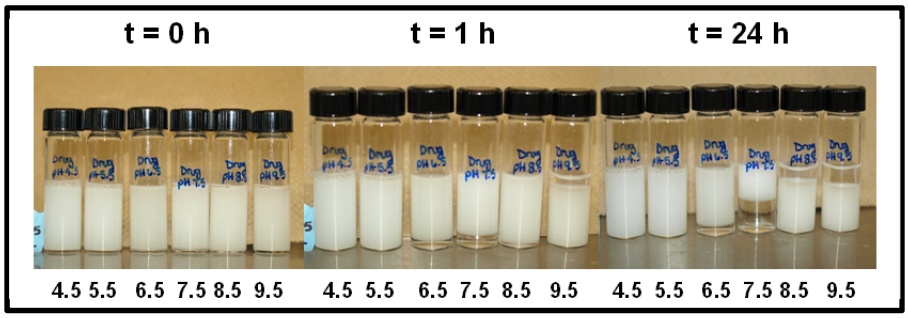

Figure 4.4. Atropine-containing particle stability in PBS for particles prepared at various aging step pH values.

However, these miniemulsion polymerization stock samples, that is the stock samples before placement in PBS, later became quite viscous and were not suitable for drug release experiments. With this observation and the lack of a homogeneously distributed particle suspension in PBS with other aging step pH

values tested, particle synthesis for all subsequent work was done using an aging step pH of 7.5.

4.2.1 Effect of polymer adsorption on particle stability in PBS for atropine-containing particles

Compared with electrostatic repulsion as a mechanism for particle stability, stabilization by adsorption of a macromolecule to the surface of a particle is independent of the ion concentration in the bulk phase. Steric stability was therefore investigated as a method for improving particle stability in a PBS solution with an ion concentration of approximately 0.3 M. Low molecular weight (8 kDa) non-ionic polyethylene glycol was previously coated onto 23-nm sized silver nanoparticles and these polymer-coated nanoparticles showed improved particle stability in 0.01 M or 0.1 M, but not 0.5 M sodium chloride (NaCl) solutions (Radziuk et al., 2007). In this work, empty and atropine-containing silica particles were incubated in various concentrations of a 4.4 kDa dimethylsiloxane polyethyleneoxide (DMS-PEO) copolymer to allow for polymer adsorption onto particles. The water soluble PEO block was expected to extend into the aqueous bulk phase, while the more hydrophobic dimethylsiloxane segment was expected to adsorb onto the particle surface. Particles incubated with DMS-PEO were then added to PBS. Samples were mixed, placed on the bench top and observed over time.

Empty and atropine-containing particles incubated with 0 (E or D), 10, 50, 100, 500, or 1000 mg/mL DMS-PEO and added to PBS are shown in **Figure 4.5.**

There was an increase in particle stability in the empty microparticles with increasing copolymer concentration at 1 h with the adsorption of DMS-PEO. Atropine-containing particle samples showed stability in PBS regardless of the copolymer concentration. In both types of samples, microparticles that were not incubated with the copolymer showed the least stability in PBS after 1 h. Improved particle stability is observed for particles incubated with the copolymer presumably because polymer adsorption onto particles results in steric stability that reduces aggregation of particles in the presence of PBS. It is noted however, that a possible increase in viscosity with increasing polymer concentrations may have also contributed to the observed improvement in particle stability.

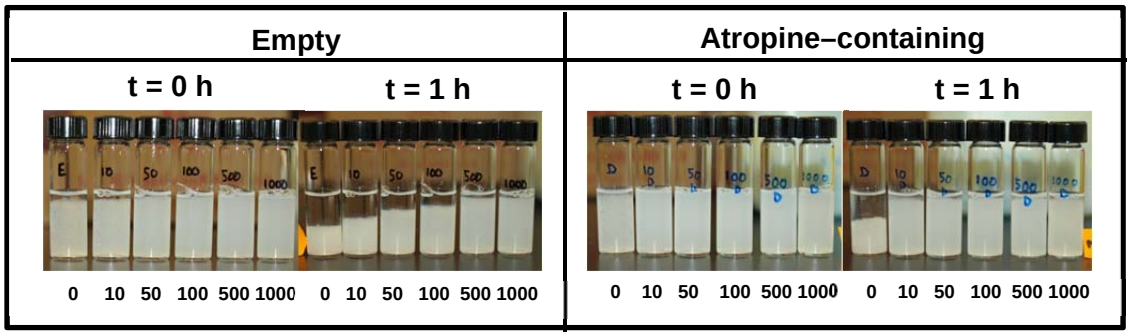

Figure 4.5. Stability of empty and atropine-containing silica particles incubated with 0, 10, 50, 100, 500, and 1000 mg/mL (w/v) 4.4 kDa DMS-PEO copolymer approximately 0 and 1 h after addition to PBS.

Electrophoretic mobility measurements were performed to evaluate polymer adsorption onto particles. As prepared silica microparticles have a negative electrophoretic mobility (**Table 4.1,** 0 mg/mL). The less negative electrophoretic mobility values observed with the adsorption of the nonionic

polymer DMS-PEO demonstrates the presence of the copolymer on the surface of particles.

Atropine-containing particles without adsorbed co-polymer were also observed to have a higher electrophoretic mobility than empty particles without adsorbed co-polymer. This might provide some insight into why atropine-containing particles show similar stability in PBS regardless of the concentration of the DMS-PEO solution that the particles were incubated in. The larger negative electrophoretic mobility value for atropine-containing particles together with a concentration, c, $0 < c \leq 10$ mg/mL DMS-PEO is sufficient for stabilizing particles over a 1 h period. Empty particles require a concentration of $100 < c \leq 500$ mg/mL DMS-PEO for particle stability for the same period of time. This suggests a potential role for atropine in controlling particle stability.

Table 4.1. Electrophoretic mobility of empty and atropine-containing silica particles incubated with increasing concentrations of DMS-PEO copolymer. Data are the mean mobility ± standard error.

DMS-PEO concentration (mg/mL) (w/v)	Electrophoretic Mobility ($x10^{-8}$ m^2/Vs)	
	Empty	Atropine-containing
0	-1.88 ± 0.26	-4.27 ± 0.09
10	-1.40 ± 0.21	-2.17 ± 0.09
50	-1.09 ± 0.06	-2.08 ± 0.08
100	-1.21 ± 0.05	-1.88 ± 0.07
500	-1.09 ± 0.06	-1.00 ± 0.06
1000	-0.51 ± 0.07	-0.89 ± 0.08

4.2.2 Effect of surfactant content on particle stability in PBS for acetazolamide-containing particles

Due to its indication for glaucoma treatment, its use as a model hydrophobic drug in Costa et al. (2010), and its lower limit of detection with UV spectrophotometry compared with atropine (**Appendix B, Figure A1 and A2**), the model drug acetazolamide was also examined with the miniemulsion technique for drug-containing silica particle synthesis.

In order to further investigate the role of surfactant content on particle stability in PBS, particles were synthesized using various weight percentages of SDS relative to TritonX-100 surfactant. The total surfactant content remained at 1% weight by volume of dH_2O as in the Pang et al. (2010) study. Therefore, the total mass of surfactant in each sample was maintained at 0.1 g. **Figure 4.6** shows the stability of particles in PBS over time, and **Figure 4.7** shows the effective particle diameter for particles synthesized using various amounts of SDS (% wt SDS/wt surfactant). As expected, the sample containing no SDS (Vial 4) showed the lowest stability due to the lack of electrostatic repulsion with the absence of the anionic SDS surfactant. Although the effective particle diameter does not seem to be affected by the SDS content, suspension in PBS seems to be influenced by the amount of SDS where samples containing higher amounts of SDS (80 and 100% wt/wt) appear to have better stability (**Figure 4.6**). The 80% and 100% SDS content miniemulsion polymerization stock samples, that is the stock samples before placement in PBS, and that containing no SDS however, were aggregated when observed at approximately six days

after synthesis compared to the other samples which still appeared colloidally stable at this time. Note that the particles in the sample containing 25% SDS (Vial 2) appear to be more stable in PBS compared to the samples prepared using the same amounts of reagents except using atropine as the hydrophobic drug (**Figure 4.4**). The sample appears to have longer stability in PBS compared with the atropine-containing sample so a later (120 h) time point is included to show aggregation of this sample in PBS does occur. This is suggestive of the amphiphilic nature of the acetazolamide drug which likely gives acetazolamide a surfactant-like property. With acetazolamide playing a surfactant-like role in the formulation, the surfactant content is increased thus contributing to increasing the particle stability in PBS. Furthermore, in PBS (pH 7.40), acetazolamide with a pKa of 7.2 (Parasrampuria, 2003) would have a fraction of molecules in ionized form giving acetazolamide a negative charge. Increasing the negative charge on the surface of particles may contribute to increasing particle stability in PBS with the acetazolamide-containing particles.

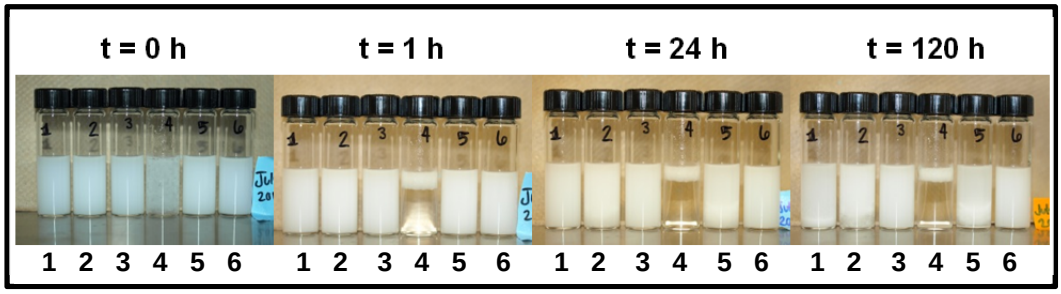

Figure 4.6. Acetazolamide-containing particle stability in PBS for particles prepared using various amounts of SDS (% wt SDS/wt surfactant). The vial numbers and their corresponding amounts of SDS (% wt SDS/wt surfactant) are listed in **Table 4.2**.

Table 4.2. SDS amounts and corresponding vial numbers.

SDS amount (% wt SDS/wt surfactant)	Vial
0	4
25	2
50	5
60	1
80	3
100	6

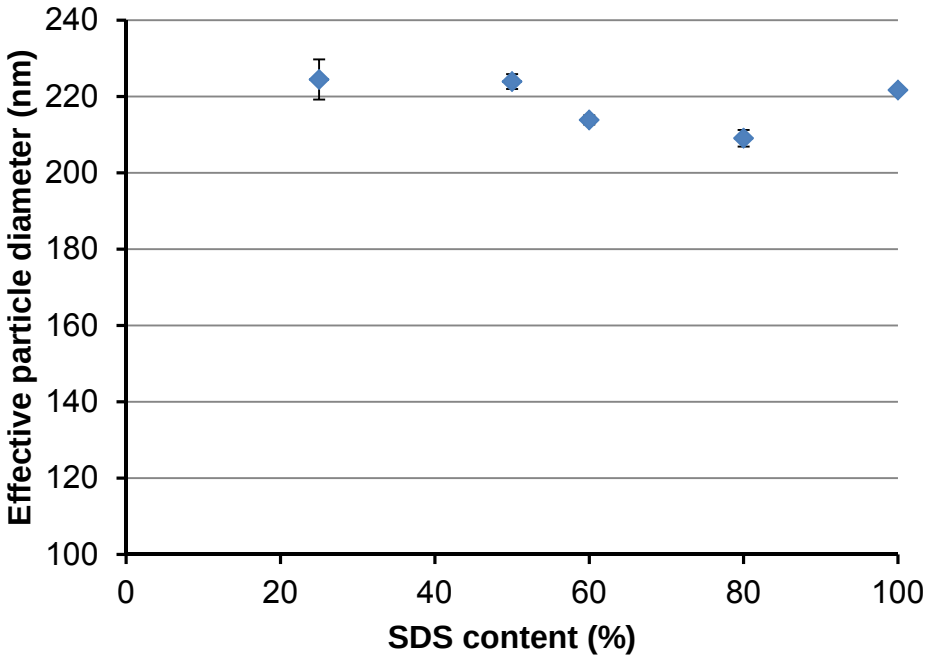

Figure 4.7. Effect of amount of SDS (% wt SDS/wt surfactant) on particle diameter. Data are the mean effective particle diameter (± SD) for three repeat measurements.

4.3 Effect of acetazolamide loading on particle diameter

In order to determine maximum loading of acetazolamide in particles with particle sizes similar to that produced previously i.e. approximately 200 nm in diameter, were synthesized with 20 mg, 200 mg and 2000 mg acetazolamide. Based on the three amounts of drug tested, the maximum drug loading in silica microparticles that allowed for a stable particle suspension was determined to be on the order of 200 mg acetazolamide (**Table 4.3**). Addition of 2000 mg acetazolamide to the oil phase for particle synthesis resulted in large measured particle diameters with a relatively larger standard deviation compared with the 20 mg and 200 mg acetazolamide-containing samples. These large diameters

are likely the result of particle aggregation due to the increased amount of drug present in the formulation. The large increase in the hydrophobic fraction of the system for the same amount of surfactant would result in areas with insufficient interfacial stabilization, leading to droplet coalescence.

Table 4.3. Effect of acetazolamide loading on particle diameter. Data are the mean effective particle diameter (± SD) for three repeat measurements.

Acetazolamide (mg)	Effective particle diameter (nm)
20	216.0 ± 0.5568
200	213.1 ± 3.236
2000	950.3 ± 151.9

4.4 Dexamethasone partitioning in oil/water for selection of internal phase oil for microemulsions

The incorporation of smaller drug-loaded nanoparticles into silicone hydrogels may be important for achieving transparency since particles larger than 100 nm in size may cause scattering of light, thus diminishing the transparency of the material. With the miniemulsion technique, drug-containing particles with a diameter of approximately 200 nm were synthesized. Therefore, in order to obtain drug-containing nanoparticles, a microemulsion polymerization technique was employed.

Using dexamethasone as the model hydrophobic drug, a microemulsion polymerization technique similar to the one described by Gulsen and Chauhan (2004) and Underhill et al. (2002) was used. Based on the measurement of the

partition coefficient, as shown in **Table 4.4**, ethyl butyrate was selected as the internal phase oil for preparation of dexamethasone-loaded silica nanoparticles.

Table 4.4. Concentration of dexamethasone in water and oils. Data are the mean ± SD for n=3.

Oil	Dexamethasone concentration in dH_2O (mg/g dH_20)	Dexamethasone concentration in oil (mg/g oil)
Isopropyl myristate	0.0186 ± 0.005	0.0208 ± 0.005
Soybean	0.0296 ± 0.008	0.00975 ± 0.008
Triacetin	0.00173 ± 0.00003	0.0376 ± 0.00003
Ethyl butyrate	0.00142 ± 0.0006	0.0379 ± 0.0006

4.5 Dexamethasone-loaded silica nanoparticle synthesis prepared by the microemulsion technique

4.5.1 Effect of dexamethasone loading

The maximum dexamethasone loading that would allow for formation of a stable particle suspension was determined to be on the order of 20 mg. Samples containing more than 20 mg of dexamethasone showed white precipitates. All subsequent microemulsions were prepared with 20 mg dexamethasone.

Table 4.5 shows particle sizes of samples prepared with 1x and 2x dexamethasone. In the sample containing no dexamethasone, it was not possible to obtain an effective particle diameter reading due to particle aggregation.

Table 4.5. Effect of dexamethasone loading on particle diameter. Data are the mean effective particle diameter (± SD) for six repeat measurements.

Relative dexamethasone content	Effective particle diameter (nm)
0	N/A
1X	82.8 ± 6.05
2X	34.7 ± 0.438

4.5.2 Effect of silica shell precursors

Drug-containing particles with MATO or TEOS as silica shell precursors, and a drug-containing microemulsion without silica shell precursors were prepared and particle sizes are shown in **Table 4.6**.

Table 4.6. Particle diameters of particles prepared with and without silica shell precursors. Data are the mean effective particle diameter (± SD) for six repeat measurements.

Microemulsion type	Effective particle diameter (nm)	
	Empty	Dexamethasone-containing
MATO	24.0 ± 0.854	31.5 ± 0.339
No shell precursor	12.8 ± 1.11	13.4 ± 0.819

The particle size measurements were taken approximately 8 days after microemulsion polymerization, while for the effect of dexamethasone loading experiment the particle size measurements were taken 15 days after synthesis. Ultimately, optimization of the chemical composition of this microemulsion system, namely the internal oil phase, the surfactant, the external water phase as

well as understanding the potential role of the drug in controlling microemulsion stability are necessary.

Note that samples were also prepared using TEOS as a silica shell precursor. However no reliable readings were obtained. This may be an indication of the delicate balance that exists between the components of this microemulsion system. The structures of MATO and TEOS are shown in *Materials and Methods*, **Figure 3.5**. It is likely that chemical differences are responsible for the differences in microemulsion stability observed. The longer methacryloxypropyl group is expected to be positioned on the particles' exterior surface, due to crosslinking between the siloxy groups of MATO and OTMS at the oil/water interface. This longer group extending from particles synthesized with MATO, but not TEOS may behave like a steric stabilizer similar to what was seen with the adsorbed polymer, thus hindering the aggregation of particles.

4.6 Characterization of HEMA/TRIS-OH silicone hydrogels embedded with dexamethasone-loaded particles

Gulsen and Chauhan (2004) described the synthesis and addition of a lidocaine-loaded silica nanoparticle microemulsion to 2-hydroxyethyl methacrylate (HEMA) to form transparent hydrogels that released lidocaine over 8 days. The addition of an aqueous particle suspension to a silicone hydrogel formulation however would presumably result in non-transparent gels due to

phase separation between the hydrophobic silicone monomer and the aqueous particle suspension.

The hydrophobic silicone monomer, 3-methacryloxypropyltris(trimethylsiloxy)silane (TRIS), does not contain hydroxyl groups (**Figure 4.8 A)**, therefore it was hypothesized that the presence of a hydroxyl group in the hydrophobic monomer such as that present in TRIS-OH **(Figure 4.8 B)** might increase miscibility of the hydrophobic monomer with the hydrophilic monomer in the presence of the aqueous microemulsions via hydrogen bonding interactions. To test this hypothesis, monomer tolerance to deionized water was qualitatively assessed by observing whether the gel formulation turned turbid after the addition of water. *N,N*-dimethylacrylamide (DMA)/TRIS, HEMA/TRIS, DMA/TRIS-OH, and HEMA/TRIS-OH at molar ratios of 90:10 hydrophilic to hydrophobic monomer content were tested. It was observed that compositions of either of the hydrophilic monomers (DMA or HEMA) and TRIS-OH tolerated more water compared to vials containing TRIS as expected. Furthermore, of the samples tested, the HEMA-TRIS-OH composition tolerated the greatest volume of water before becoming turbid. Therefore, the HEMA-TRIS-OH (90:10) monomers were selected for preparation of silicone hydrogels embedded with dexamethasone-containing silica particles.

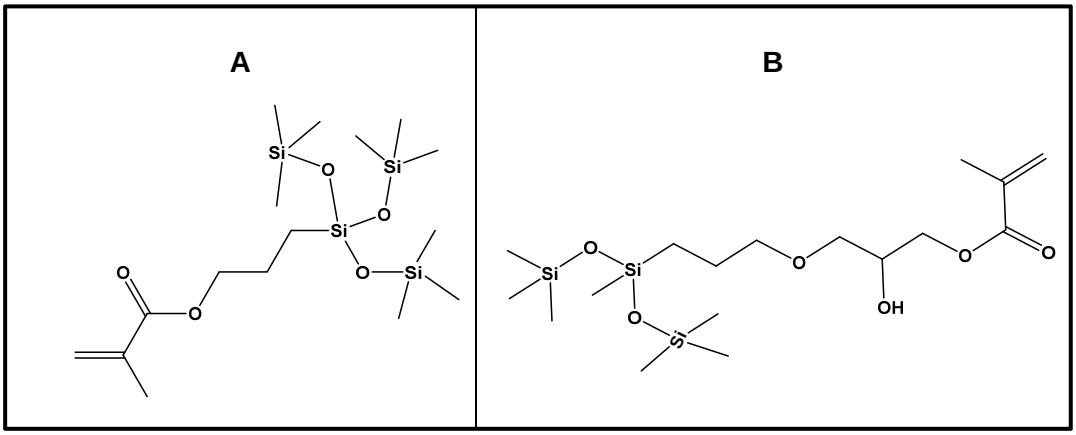

Figure 4.8 (A). TRIS and **(B).** TRIS-OH.

4.6.1 Equilibrium water content

4.6.1.1 Effect of dexamethasone loading

The water content of commercially available contact lenses ranges between 24% to 74% (Contact lens spectrum, 2012). The equilibrium water content of the HEMA/TRIS-OH (90:10) silicone hydrogel materials embedded with particles was measured and is listed in **Table 4.7** and **Table 4.8**. The equilibrium water content of all the HEMA/TRIS-OH (90:10) materials was approximately 32%.

Table 4.7. Equilibrium water content for HEMA/TRIS-OH gels embedded with silica nanoparticles containing 0, 1x, or 2x dexamethasone. Data are the mean (± SD) for n=6.

Relative dexamethasone content	EWC (%)
0	32.0 ± 0.668
1x	31.7 ± 1.13
2x	31.9 ± 0.816

4.6.1.2 Effect of silica shell precursors

Table 4.8. Equilibrium water content for HEMA/TRIS-OH disks embedded with particles prepared with and without silica shell precursors and with or without dexamethasone. Data are the mean (± SD) for n=6.

Microemulsion type	EWC (%)	
	Empty	Dexamethasone-containing
MATO	31.5 ± 0.793	32.4 ± 0.912
TEOS	31.6 ± 0.326	31.7 ± 0.450
No silica shell precursors	31.1 ± 0.571	30.6 ± 1.02

An equilibrium water content study was also done with HEMA/TRIS-OH and HEMA/TRIS-OH disks embedded with dexamethasone-containing particles prepared with MATO silica shell precursor (MATO/D) disks as shown in **Table 4.9**. The HEMA/TRIS-OH disks had a lower mean equilibrium content than MATO/D disks. The HEMA/TRIS-OH hydrogel was prepared by polymerization of HEMA and TRIS-OH monomers in the absence of water. The particle-embedded HEMA/TRIS-OH hydrogels, however were polymerized in the presence of water, which diluted the overall molar concentrations of monomer and crosslinker in the gel formulation. This would reduce the crosslink density of

the hydrogel matrix thus allowing for increased water penetration into the hydrogel matrix. Bajpai and Singh (2006) also attributed increased swelling of hydrogels prepared by dilution of the reaction mixture with water to decreased crosslinking within the polymer matrix.

Table 4.9. Equilibrium water content for HEMA/TRIS-OH disks and MATO/D disks. Data are the mean (± SD) for n=6.

Disk type	EWC (%)
HEMA/TRIS-OH	23.1 ± 1.21
MATO/D	31.1 ± 0.954

4.6.2 Transparency

Transmittance measurements were performed for swollen HEMA/TRIS-OH (90:10) disks to evaluate the transparency of these materials. Based on visual examination of the swollen disks, as well as the transmittance values seen in **Figure 4.9** and **Figure 4.10** the disks are not sufficiently transparent to be suitable for lens wear. The presence of the aqueous microemulsion in the HEMA/TRIS-OH gel formulation likely causes phase separation of pHEMA and silicone domains during polymerization leading to a reduction in the material transparency. The disk thickness of measured lenses were approximately 0.5 mm, while commercial contact lenses are approximately 0.1 mm. A reduction in the disk thickness may increase transparency.

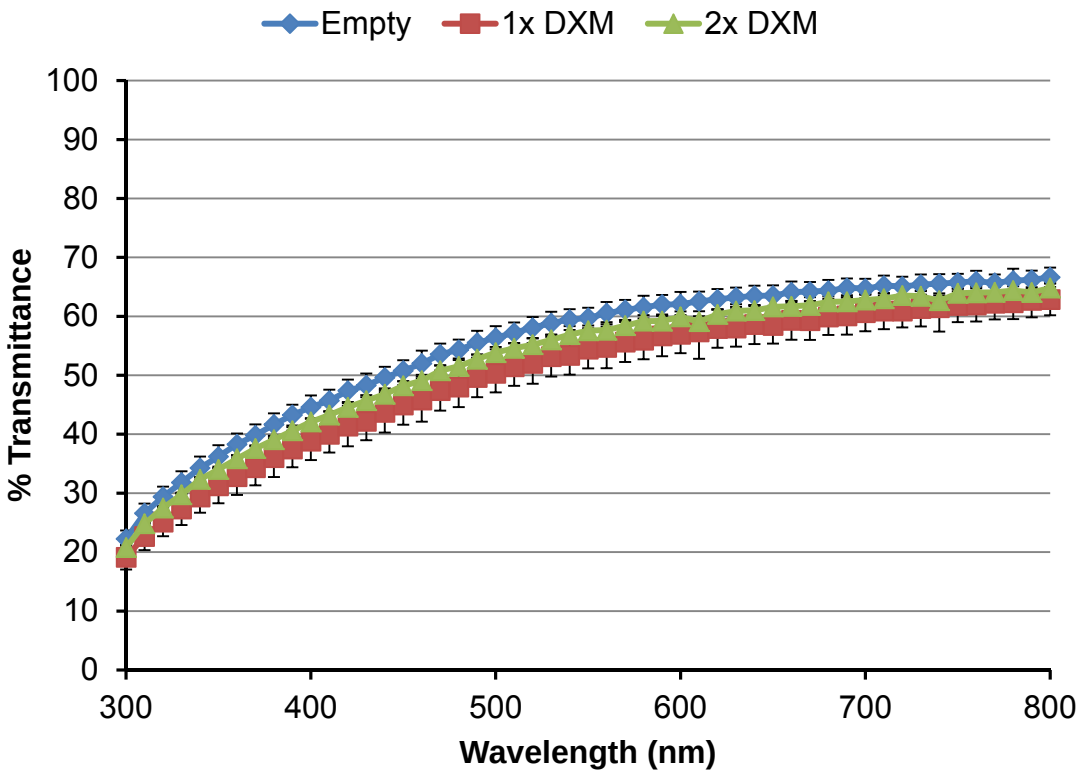

Figure 4.9. % transmittance for HEMA/TRIS-OH gels embedded with silica nanoparticles containing 0, 1x, or 2x dexamethasone (DXM). % transmittance values are the mean (± SD) for n=6.

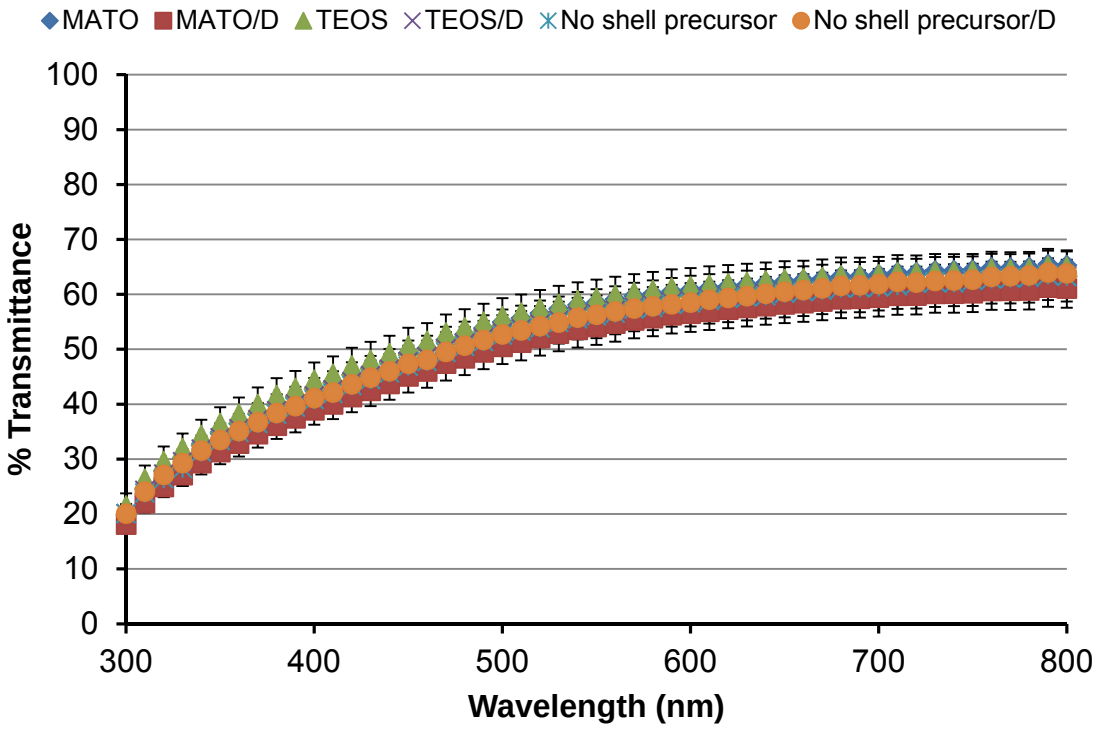

Figure 4.10. % transmittance for HEMA/TRIS-OH gels embedded with particles prepared with and without silica shell precursors and with or without dexamethasone (DXM). % transmittance values are the mean (± SD) for n=6.

A transparency study was also done with HEMA/TRIS-OH and MATO/D disks, and as shown in **Figure 4.11**, HEMA/TRIS-OH disks are more transparent than the HEMA/TRIS-OH hydrogel disks embedded with dexamethasone-containing particles.

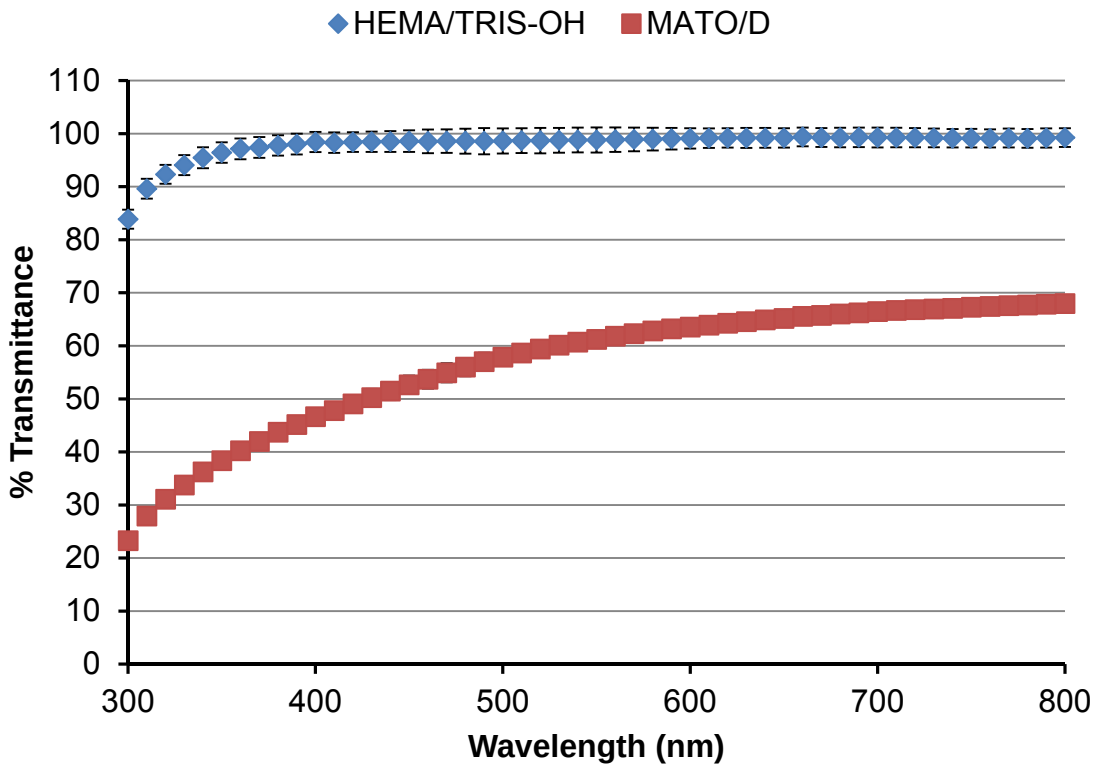

Figure 4.11. % transmittance for HEMA/TRIS-OH disks and MATO/D disks. % transmittance values are the mean (± SD) for n=6.

4.6.3 Transmission electron microscopy (TEM) for particle visualization

Transmission electron microscopy was employed in order to examine particle localization within the material and to be able to view the HEMA and TRIS-OH regions in order confirm phase separation as the cause for reduced material transparency.

HEMA/TRIS-OH (90:10) hydrogels embedded with dexamethasone-containing particles were sectioned in the dry state for TEM analysis. **Figure 4.12** are micrographs of silicone hydrogels embedded with dexamethasone-

containing particles with MATO as the silica shell precursor. Micrographs taken at increasing magnifications are for a region within the gel containing what appears to be silica nanoparticles. Due to relative ratios of darker to lighter regions, the darker continuous region is believed to be the pHEMA domain, while the lighter network-like domain is believed to be the silicone domain. Light and dark contrast regions are also seen in TEM micrographs of hydroxyl terminated polydimethyl siloxane/poly N-isopropyl acrylamide interpenetrating networks (Liu and Sheardown, 2005). Furthermore, the darker regions in the HEMA/TRIS-OH hydrogels with embedded particles were less sensitive to the electron beam during TEM imaging similar to HEMA and HEMA/dH_2O samples (**Appendix B, Figure A3 and Figure A4**). The lighter domains of the gel were more sensitive to the electron beam and were prone to ripping as can be seen as holes in the TEM images for HEMA/TRIS-OH hydrogels embedded with dexamethasone-containing particles. The existence of these two clearly distinguishable regions at the microscopic level is suggestive of the phase separation that occurred during polymerization in the presence of an aqueous particle suspension in the gel formulation. These domains are larger than the wavelength of visible light and would cause the scattering of light, decreasing light transmission through the material creating a material with low transparency.

The darker contrast spots situated along the supposed silicone network are believed to be silica nanoparticles. The silica particles were hypothesized to partition in the silicone domain due to interactions between silicone groups on the

particle surface and in the TRIS-OH monomer. It was expected that partitioning of the particles in the silicone domain of the hydrogel matrix might contribute to a slower drug release rate since the silicone domain would have reduced access to the water channels present in the hydrophilic HEMA domain.

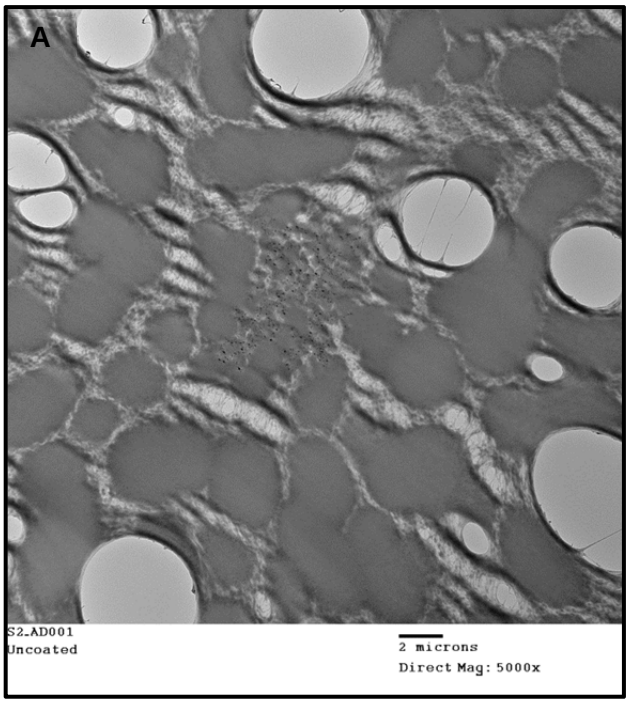

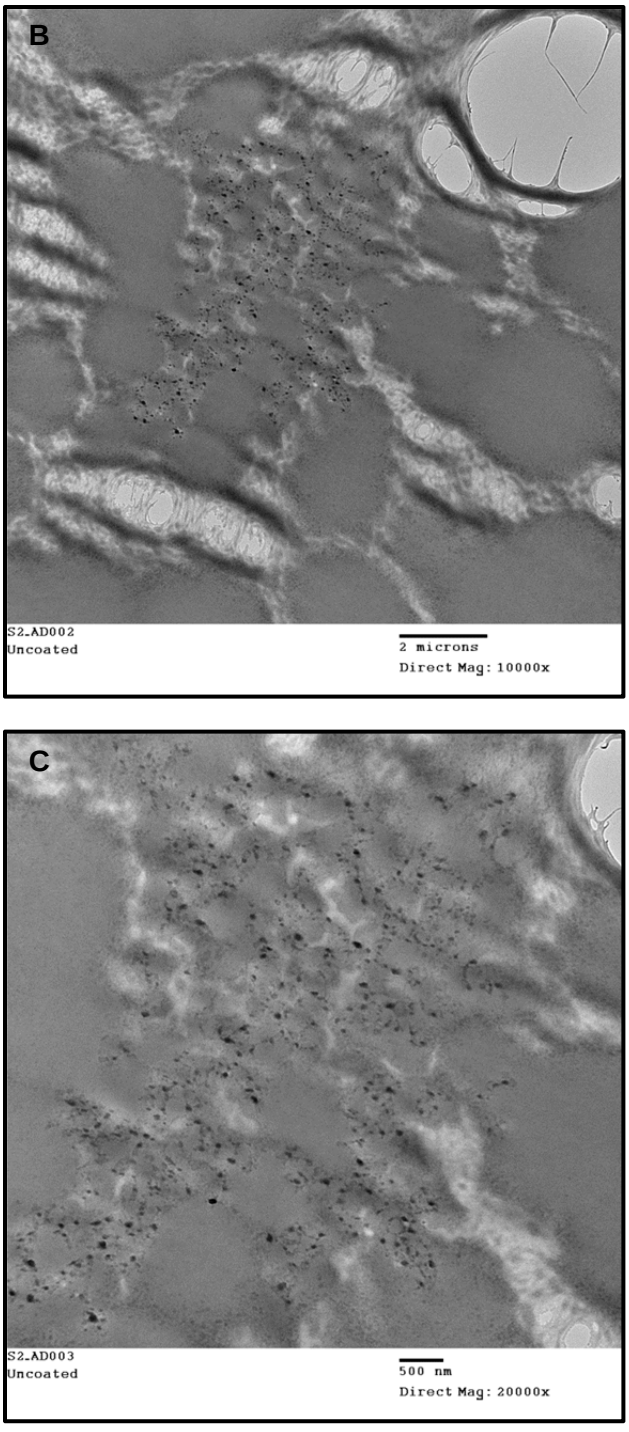

Figure 4.12. TEM micrographs of HEMA/TRIS-OH (90:10) hydrogel embedded with dexamethasone-containing particles with MATO as silica shell precursor. The three micrographs are a section of the hydrogel viewed at **(A)** 5000x, **(B)** 10,000x, and **(C)** 20,000x magnification. The scale bar is 2 μm for **(A)** and **(B)**, and 500 nm for **(C).**

The HEMA/TRIS-OH hydrogel embedded with particles prepared with TEOS as a silica shell precursor also had particles that localized in the TRIS-OH domain (**Figure 4.13**). The morphology of these particles compared with MATO particles, appeared more irregular and clustered. As mentioned previously, this may be due to the instability of particles prepared with TEOS as the shell precursor. Similar dark spots were not seen in HEMA/TRIS-OH hydrogels embedded with particles prepared with no silica shell precursors.

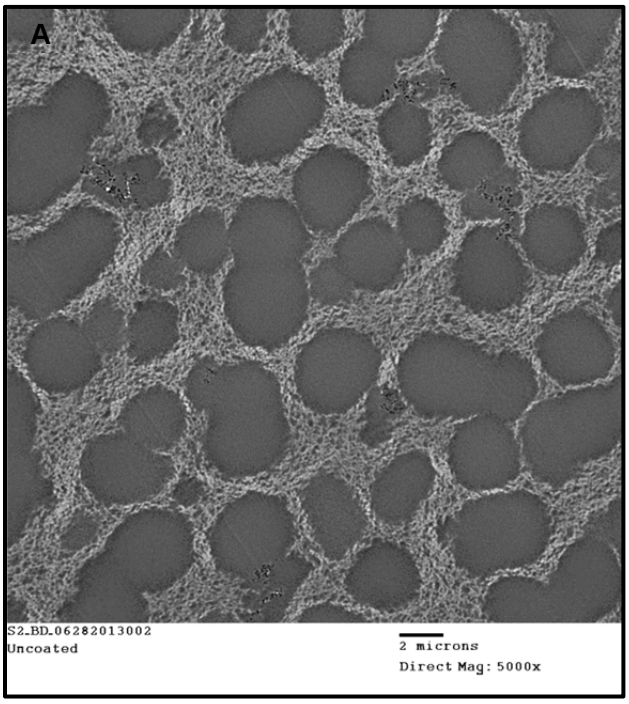

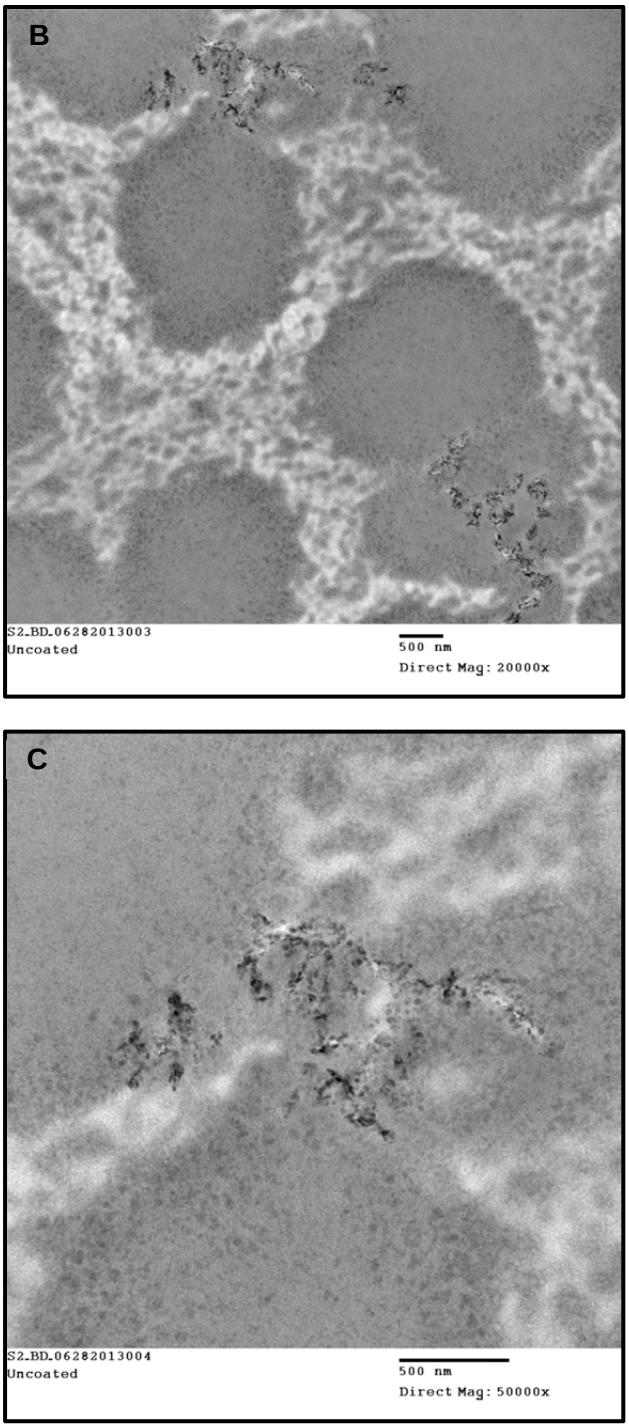

Figure 4.13. TEM micrographs of HEMA/TRIS-OH (90:10) hydrogel embedded with dexamethasone-containing particles with TEOS as silica shell precursor. The three micrographs are a section of the hydrogel viewed at **(A)** 5000x, **(B)** 20,000x, and **(C)** 50,000x magnification. The scale bar is 2 μm for **(A)**, and 500 nm for **(B)** and **(C)**.

4.6.3.1 TEM of dexamethasone-containing particle suspensions

In order to investigate whether the darker contrast spots in the silicone domains are indeed silica particles, microemulsion polymerizations using MATO, TEOS or no shell precursors were done and the suspensions were visualized by TEM. Dark contrast spherical particles appear to be present in all three samples (**Figure 4.14 A**, **4.14 B**, **4.14 C**). The microemulsion to which no silica precursor was added seemed to have clusters of colloidal particles. A silica shell around particles may allow for increased particle stability, decreasing particle aggregation. As mentioned earlier, dark contrast spots were not visible in HEMA/TRIS-OH hydrogels embedded with microemulsions prepared without silica shell precursors. The absence of a silica shell around particles may lead to a destabilization of the microemulsions droplets stabilized by Brij 97 surfactant when this suspension is added to the gel formulation explaining the absence of dark spots in this hydrogel sample.

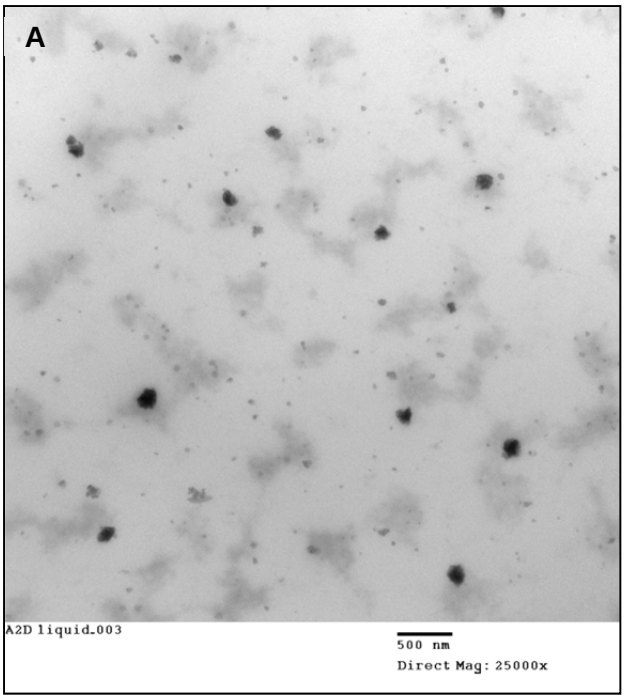
A
A2D liquid_003
500 nm
Direct Mag: 25000x

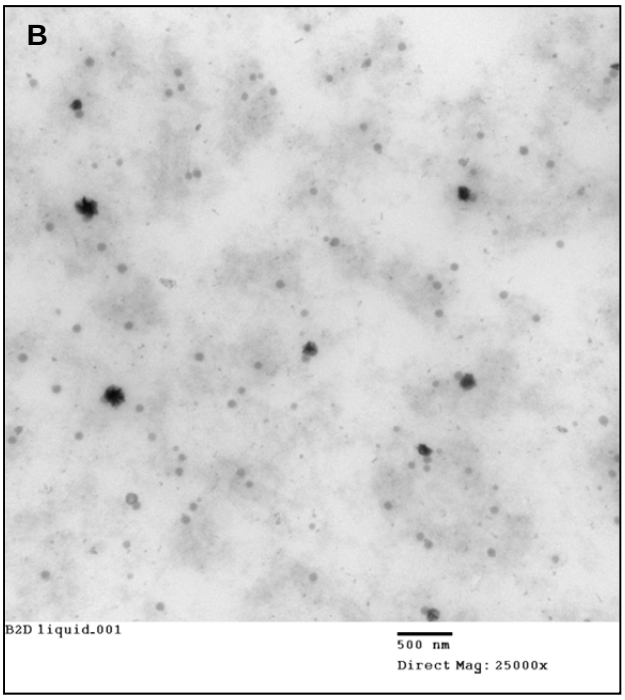
B
B2D liquid_001
500 nm
Direct Mag: 25000x

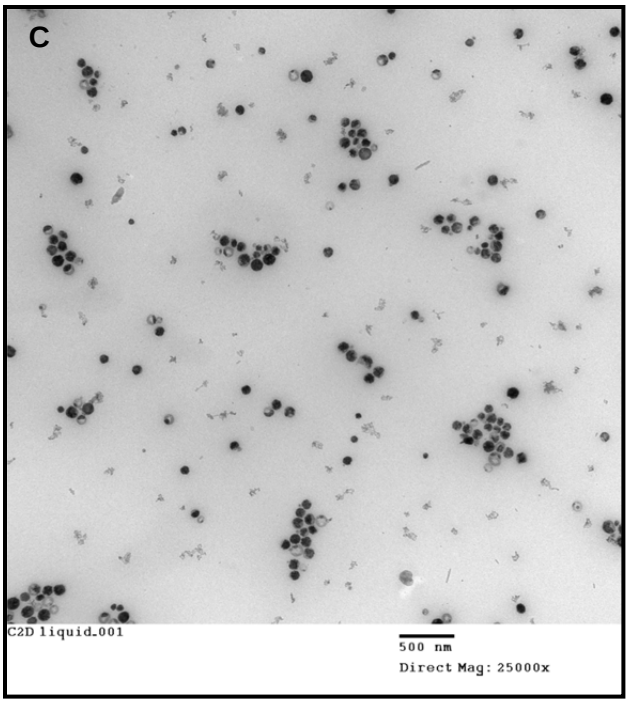

Figure 4.14. TEM micrographs of dexamethasone-containing nanoparticles with **(A)** MATO silica shell precursor, **(B)** TEOS silica shell precursor, and **(C)** no silica shell precursor. Particles at 25,000x magnification. The scale bar is 500 nm.

4.7 Dexamethasone release from HEMA/TRIS-OH silicone hydrogels embedded with dexamethasone-loaded silica particles

Dexamethasone release from HEMA/TRIS-OH disks embedded with dexamethasone-containing particles was conducted at 34°C in PBS over a period of 28 days. Release studies were conducted to observe release profiles from silica particles containing different loadings of dexamethasone, and to observe whether the inclusion of silica shell precursors in the microemulsion formulation affects the release profile. A roughly constant rate of release for both studies was observed for approximately five days.

4.7.1 Effect of dexamethasone loading

Release was dependent loading; the average cumulative release for the 2x dexamethasone sample was 0.32 ± 2.2x10^{-6} µg dexamethasone/mg dry disk mass, while that of the 1x dexamethasone sample was 0.17 ± 1.6 x10^{-6} µg dexamethasone/mg dry disk mass (**Figure 4.15**). Based on the amount of dexamethasone loaded per disk mass, taking into account the dexamethasone loss during gel soaking prior to punching out disks, the 1x and 2x samples released 90% and 92% of the dexamethasone loaded respectively.

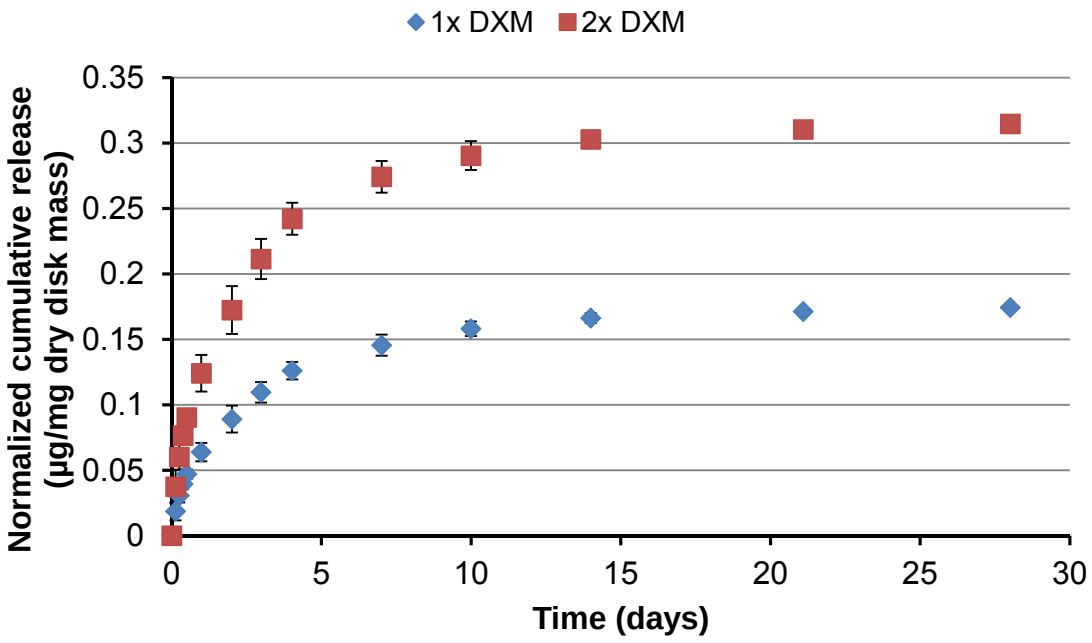

Figure 4.15. Dexamethasone (DXM) release in PBS at 34°C from silica nanoparticles containing 1x and 2x dexamethasone. Normalized cumulative release values are the mean (±SD) for n = 6.

4.7.2 Effect of silica shell precursors

HEMA/TRIS-OH disks embedded with particles prepared with MATO, TEOS, or no shell precursor had similar release profiles **(Figure 4.16)**. ANOVA analysis of the results suggests no statistical difference between the sample types for release of dexamethasone ($p>0.05$). The average normalized cumulative release values for the MATO, TEOS, and no shell precursor samples were $0.33\pm 5.0 \times 10^{-6}$ µg, $0.33 \pm 3.3 \times 10^{-6}$ µg, and $0.31 \pm 3.7 \times 10^{-6}$ µg per mg dry disk mass respectively. The total dexamethasone release based on the calculated amount of dexamethasone loaded into the gels was 93%, 92%, and 87% for the MATO, TEOS, and no shell precursor samples respectively.

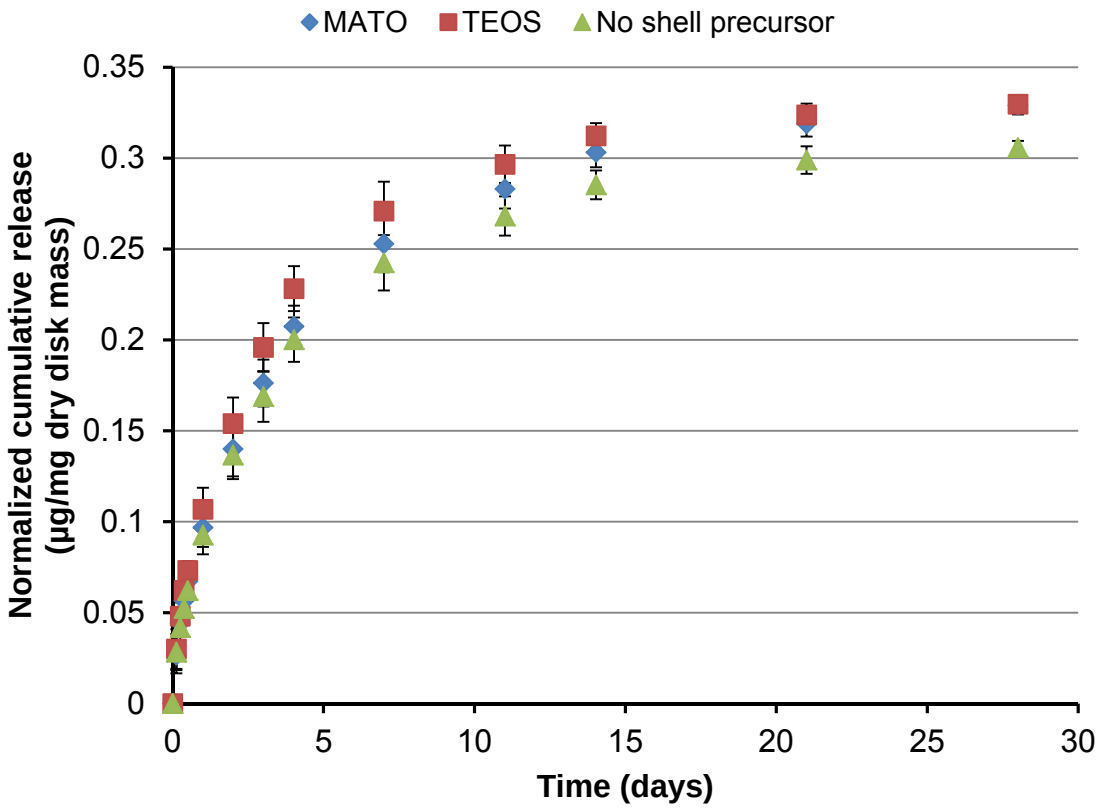

Figure 4.16. Dexamethasone release into PBS at 34°C from HEMA/TRIS-OH disks embedded with particles synthesized with MATO, TEOS, or no shell precursor. Normalized cumulative release values are the mean (±SD) for n=6.

Gulsen and Chauhan (2004) reported similar release profiles for pHEMA gels embedded with particles synthesized using OTMS as the silica shell precursor and with microemulsion droplets. It was hypothesized that the use of an additional silica shell precursor, TEOS, would result in a more stable silica shell on particles compared with using OTMS alone and would result in a slowed release rate. Additionally, it was expected that using an alternate silica shell precursor, MATO, with an acryl group in its chemical structure may result in the

formation of chemical bonds between particles' silica shell and the hydrogel matrix. If the drug-containing silica particles were located in the silicone domain of the hydrogel matrix and were immobilized there by chemical bonds, a slower rate of drug release would be expected due to limited access to water channels in the silicone domains. This was not observed however, as the hydrogel embedded with particles without silica shell precursors showed a similar release rate to those embedded with particles prepared with silica shell precursors. This is consistent with TEM results. If diffusion from particles rather than diffusion from the hydrogel matrix is the rate controlling mechanism for drug release then it appears that a microemulsion system stabilized with Brij 97 surfactant may be sufficient for controlling the drug release behaviour. The TEM micrograph showing colloidal structures in the particle suspensions without silica shell precursors, but an absence of these particles in the hydrogel suggests that unencapsulated dexamethasone might be present in the hydrogels due to a destabilization of the surfactant-stabilized droplets upon addition to the gel formulation. Since dexamethasone release for the three hydrogel types was similar, release may be controlled by diffusion of free dexamethasone from the gel matrix. If this is the case, dexamethasone was not sufficiently encapsulated within silica nanoparticles or release from the particles occurred quickly and encapsulation within silica particles was not rate limiting for dexamethasone release.

4.8 Mechanism of drug release for hydrogels embedded with drug-containing particles

In order to investigate whether drug release from a hydrogel is controlled by diffusion from the hydrogel matrix, investigators observe release profiles from gels of various thicknesses (Kim et al., 2008; Lu et al., 2012). With this experiment, drug release into PBS is done until an equilibrium drug concentration is reached. If diffusion is the rate limiting mechanism for drug release, a gel with twice the thickness, while maintaining the same fluid to gel volume ratio, will have a release time scale that is four times that of a gel that is half as thick. Other mechanisms such as drug adsorption and desorption or channel formation might be contributing to the drug release profile if the release time scale is less than four times that of a gel that is half as thick (Kim et al., 2008). Alternatively, the normalized drug release (drug release mass/dry gel mass) for the gels of different thicknesses may be plotted against a scaled time **(4.1)** axis, or cumulative percent release may be plotted against scaled time, τ **(4.2)**. If the profiles of gels with different thicknesses overlap, release from the gel is dependent on gel thickness, and diffusion from the gel matrix controls the release behaviour.

$$Scaled\ time\ for\ gel\ of\ thickness\ b = \frac{time}{\frac{b^2}{a}} \quad \textbf{(4.1)}$$

$$\tau = \sqrt{\frac{time}{\frac{b^2}{a}}} \quad \textbf{(4.2)}$$

a is the thickness of the thin gel and *b* is the thickness of the thicker gel. A similar experiment may be conducted to investigate whether the presence of drug-containing particle systems might play a role in controlling the drug release profile. For instance, in order to determine whether the drug release rate for pHEMA hydrogels embedded with silica shell cross-linked micelles is limited by drug diffusion from the gel matrix, the percent cumulative dexamethasone acetate release verses τ was plotted (Lu et al., 2012). The drug release was determined to be independent of gel thickness, and therefore diffusion from silica shell cross-linked micelles was concluded to be the rate limiting factor for drug release.

When preparing silicone hydrogels with embedded drug-containing particles by the addition of a particle suspension to the gel formulation, it is possible that a portion of the drug will not be encapsulated within particles. If drug release is controlled by drug diffusion from the particles, then the amount of drug loading within particles may be calculated by comparing the release from gels of different thicknesses. Since the mechanism of release for the unencapsulated drug would be diffusion through the gel matrix, the normalized release versus scaled time for gels of two different thicknesses will have overlapping drug release profiles during this initial period of release. This would then be followed by a second phase of drug release during which the graphs do not overlap indicating the period of drug release due to diffusion from particles. The total mass of encapsulated drug may then be approximated by subtracting

the mass of drug released during the initial phase of release from the initial amount of drug loaded. This type of analysis may be useful for the evaluation of methods to optimize drug encapsulation efficiency.

5. CONCLUSIONS AND RECOMMENDATIONS

5.1 Conclusions

In this work, drug-containing silica particles were prepared using miniemulsion and microemulsion polymerization methods. Stability of particles in PBS prepared using the miniemulsion polymerization technique was investigated by varying the aging step pH, using various ratios of anionic to non-ionic surfactant, or by polymer adsorption. Varying the aging step pH and the ratio of surfactants may result in particle suspensions that are not colloidally stable over time. Polymer adsorption onto particles can be used to increase colloidal stability.

HEMA/TRIS-OH silicone hydrogels embedded with drug-containing silica particles were prepared. A hydroxylated silicone monomer, compared with a silicone monomer that did not contain a hydroxyl group, tolerated more water before phase separation occurred in the presence of the hydrophilic HEMA monomer. Drug-containing particles were prepared using a microemulsion polymerization technique. The gel formulation containing the aqueous particle suspension was a transparent solution, however curing of the formulation resulted in silicone hydrogels that were not transparent. HEMA/TRIS-OH gels were transparent; the presence of water in the silicone hydrogel formulation likely causes separation of the hydrophilic pHEMA and silicone domains during polymerization. Silicone domains in HEMA/TRIS-OH gels embedded with drug-containing particles were larger than 100 nm in size as observed by transmission

electron microscopy. These large domains in the hydrogel may cause light refraction which would consequently result in decreased light transmittance.

Drug release experiments with HEMA/TRIS-OH gels embedded with dexamethasone-containing particles showed a concentration-dependent release profile where gels containing particles loaded with approximately twice the amount of dexamethasone released approximately twice the amount of the drug. Two distinct domains were present in HEMA/TRIS-OH gels containing particles. These were a darker continuous region believed to be the pHEMA domain due to the higher proportion in the gel formulation and lesser sensitivity to the electron beam, and lighter regions believed to be silicone (TRIS-OH) domains. Particles prepared with MATO and TEOS as silica shell precursors appeared to be sequestered in this lighter silicone domain presumably due to interactions between the particles' silica shell and the silicone domains. Upon viewing colloidal structures in particle suspensions containing MATO, TEOS, or no shell precursor, the absence of similar structures in the TEM micrographs of hydrogels containing suspensions to which no silica shell precursor was added suggests a possible role of silica shell precursors in stabilizing particles and localizing these drug-containing vehicles to the silicone domains of the hydrogel matrix. Comparing silicone hydrogels incorporated with suspensions prepared using MATO verses TEOS as a silica shell precursor, MATO particles appear to be more spherical in shape compared with TEOS particles. The chemical structure of MATO might contribute to improved particle stability in MATO particles in

comparison with TEOS particles. Taking results of the drug release data and TEM micrographs together, the similar release profiles for hydrogels composed of particle suspensions containing MATO, TEOS, or no shell precursors suggests that the release mechanism was likely due to diffusion of dexamethasone from the hydrogel matrix, and that the silica shell on particles did not offer significant resistance to drug diffusion.

5.2 Recommendations for future work

Despite similar release profiles observed for silicone hydrogels incorporated with suspensions prepared with and without silica shell precursors, the particle localization in the silicone domains observed for hydrogels embedded with particles containing a silica shell is promising for potentially obtaining slow release from the silicone domains. Optimizing the amount of silica shell precursors added to the microemulsion may be useful for investigating whether the quantity of the silica precursors influences the release profile compared with particles prepared without silica shell precursors.

Furthermore, gels embedded with drug-containing particles should be prepared with varying thicknesses to validate that diffusion from the hydrogel matrix, as opposed to another mechanism, is the rate controlling mechanism for drug release. If the graphs of normalized release verses scaled time for gels of different thicknesses do not overlap, the presence of particles may be contributing to the release rate of dexamethasone from the silicone hydrogel.

The silicone monomer employed for silicone hydrogel preparation in this study consisted of a single hydroxyl group. The presence of the hydroxyl group in the monomer likely increased the tolerance of the gel formulation to phase separation due to hydrogen bonding between the hydroxyl groups in the hydrophobic monomer and water molecules of the aqueous particle suspension. Using a silicone monomer with more hydroxyl groups may increase the amount of the aqueous particle suspension that may be added prior to phase separation. This would increase the particle loading in the gel formulation. Alternatively as was done by Lu et al. (2013), the aqueous particle suspension may be concentrated by adding the particle suspension to dialysis tubing and placing the dialysis bag on a bed of polyethylene glycol powder which would absorb water and decrease the water content in the particle suspension.

6. REFERENCES

Ahola, M.S.,E.S. Säilynoja, M.H. Raitavuo, M.M. Vaahtio, J.I. Salonen, A.U.O. Yli-Urpo, “In vitro release of heparin from silica xerogels,” Biomaterials, 22, 2163-2170 (2001).

Alvarez-Lorenzo, C., H. Hiratani and A. Concheiro, “Contact lenses for drug delivery,” Am. J. Drug. Deliv., 4, 131–151 (2006).

Ambroziak, A, J.P. Szaflik, J. Szflik, “Therapeutic use of a silicone hydrogel contact lens in selected clinical cases.” Eye Contact Lens, 30, 63–67 (2004).

Bajpai, S.K., and S. Singh, “Analysis of swelling behaviour of poly(methacrylamide-co-methacrylic acid) hydrogels and effect of synthesis conditions on water uptake,” React. Funct. Polym., 66, 431-440 (2006).

Balasubramaniam, J., S. Kant, J.K. Pandit, “In vitro and in vivo evaluation of the gelritegellan gum-based ocular delivery system for indomethacin”, ActaPharma. 53, 251–261 (2003).

Barbé, C., J. Bartlett, L. Kong, K. Finnie, H. Q. Lin, M. Larkin, S. Calleja, A. Bush, and G. Calleja, “Silica particles: a novel drug-delivery system,” Adv. Mater., 16,1959-1966 (2004).

Barbé, C.J., Kong, L, Finnie, K.S., Calleja, S., Hanna, J.V., Drabarek, E., Cassidy, D.T., Blackford, M.G., “Sol-gel matrices for controlled release: from macro to nano using emulsion polymerisation,” J. Sol-Gel Sci. Technol., 46, 393-409 (2008).

Berkland, C., K. Kim, D.W. Pack, “PLG microsphere size controls drug release rate through several competing factors.” Pharm. Res. 20, 1055–1062 (2003a).

Berkland, C., M.J. Kipper, B. Narasimhan, K. Kim, D.W. Pack, “Microsphere size, precipitation kinetics and drug distribution control drug release from biodegradable polyanhydride microspheres.” J. Controlled. Release. 94, 129–141 (2004b).

Boone, A., A. Hui, and L. Jones, “Uptake and release of dexamethasone phosphate from silicone hydrogel and group I, II, and IV hydrogel,” Eye Contact Lens, 5, 260-267 (2009).

Boninsegna, S., P. Bosetti, G. Carturan, G. Dellagiacoma, R. Dal Monte, M. Rossi, “Encapsulation of individual pancreatic islets by sol/gel SiO2: A novel procedure for perspective cellular grafts,” J. Biotechnol. 2003, 100, 277-286.

“Glaucoma.” The Canadian National Institute for the Blind. www.cnib.ca (2013).

Carturan, G., M. Muraca, R. Dal Monte, “Encapsulation of supported animal cells using gas-phase inorganic alkoxides,” US Patent 6,214,593 (2001).

Cascone, M.G., Z. Zhu, F. Borselli, L. Lazzeri, “Poly(vinyl alcohol) hydrogels as hydrophilic matrices for the release of lipophilic drugs loaded in PLGA nanoparticles,” J. Mater. Sci.:Mater. Med. 13, 29-32 (2002).

Chua, W.-H, V. Balakrishnan, Y.-H. Chan, L. Tong, Y. Ling, B.-L. Quah, D. Tan, “Atropine for the treatment of childhood myopia,” Ophthalmology, 113, 2285-2291 (2006).

Cihlar, J., “Hydrolysis and polycondensation of ethyl silicates.1. Effect of pH and catalyst on the hydrolysis and polycondensation of tetraethoxysilane (TEOS),” Colloids Surf., A. 70, 239-251 (1993).

Ciolino, J.B., C.H. Dohlman, D.S. Kohane, “Contact lenses for drug delivery,” Semin. Ophthalmol., 24, 156–160 (2009).

Contact lens spectrum, “Soft contact lenses: hydrogel and silicone hydrogel lens general considerations,” Contact Lens Spectrum, 27, 5-23 (2012).

Costa, V.P., M.E.M. Braga, C.M.M. Duarte, C. Alvarez-Lorenzo, A. Concheiro, M.H. Gil, H.C. de Sousa, “Anti-glaucoma drug-loaded contanct lenses prepared using supercritical solvent impregnation,” J. Supercrit. Fluids, 53, 165-173 (2010).

Creech, J.L., A. Chauhan, C.J. Radke, “Dispersive mixing in the posterior tear film under a soft contact lens,” Ind. Eng. Chem. Res., 40, 3015-3026 (2001).

Curran, M.D. and A.E. Stiegman, “Morphology and pore structure of silica xerogels made at low pH,” J. Non-Cryst. Solids, 249, 62-68 (1999).

Danhier, F., O. Feron, V. Préat, “To exploit the tumor microenvironment: Passive and active tumor targeting of nanocarriers for anti-cancer drug delivery,” J. Controlled Release. 148, 135-146 (2010).

Danion, A., I. Arsenault, P. Vermette, “Antibacterial activity of contact lenses bearing surface-immobilized layers of intact liposomes loaded with levofloxacin,” J. Pharm. Sci. 96, 2350-2363 (2007).

Del Valle, E.M.M., “Cyclodextrins and their uses: a review,” Process Biochem. 39, 1033-1046 (2004).

dos Santos, J-F.R., C. Alvarez-Lorenzo, M. Silva, L. Balsa, J. Couceiro, J-J. Torres-Labandeira, A. Concheiro, “Soft contact lenses functionalized with pendant cyclodextrins for controlled drug delivery,” Biomaterials. 30, 1348-1355 (2009).

Eisenberg, D.L. C.B. Toris, C.B.Camras, “Bimatoprost and travoprost: A review of recent studies of two new glaucoma drugs”. Surv. Ophthalmol. 47 (suppl 1): S105-S115 (2002).

El-Kamel, A.H., “In vitro and in vivo evaluation of pluronic F127-based ocular delivery system for timolol maleate,” Int. J. Pharm. 241 47–55 (2002).

Gana, L., Y. Gan, C. Zhub, X. Zhang, J. Zhu, “Novel microemulsion in situ electrolyte-triggered gelling system for ophthalmic delivery of lipophilic cyclosporine A: in vitro and in vivo results,” Int. J. Pharm. 365, 143–149 (2009).

The Glaucoma Research Society of Canada. www.glaucomaresearch.ca (2013)

Gulsen, D., and A. Chauhan, “Ophthalmic drug delivery through contact lenses,” Invest. Ophthalmol. Vis. Sci. 45, 2342-2347 (2004).

Gulsen, D, C-C. Li, and A. Chauhan, “Dispersion of DMPC liposomes in contact lenses for ophthalmic drug delivery,” Curr. Eye Res. 20, 1071-1080 (2005).

Gupta, S. and S.P. Vyas, “Caebopol/chitosan based pH triggered in situ gelling system for ocular delivery of timolol maleate,” Sci. Pharm. 78, 959–976 (2010).

Hoare, T. and D. Kohane, “Hydrogels in drug delivery: Progress and challenges,” Polymer. 49, 1993-2007 (2008).

Ibrahim, H., C. Bindschaedler, E. Doelker, P. Buri, R. Gurny, “Concept and development of ophthalmic pseudo-latexes triggered by pH,” Int. J. Pharm. 77 211–219 (1991).

Iruzubieta, J.M., Ripoll, J.R.N., Chiva, J., Fernándes, O.E., Alvarez, J.J.R., Delgado, F., Villa, C., and Traverso, L.M., “Practical experience with a high Dk

lotrafilcon A fluorosilicone hydrogel extended wear contact lens in Spain," CLAO J. 27, 41-46 (2001).

Kim, J. and A. Chauhan, "Dexamethasone transport and ocular delivery from poly (hydroxyethyl methacrylate) gels," Int. J. Pharm. 353, 205–222 (2008).

Kim, J., A. Conway, and A. Chauhan, "Extended delivery of ophthalmic drugs by silicone hydrogel contact lenses," Biomaterials. 29, 2259–2269 (2008).

Järvinen, K., T. Järvinen, A. Urtti, "Ocular absorption following topical delivery," Adv. Drug Delivery Rev. 16, 3-19 (1995).

Jung, H.J., M. Abou-Jaoude, B.E. Carbia, C. Plummer and A. Chauhan, "Glaucoma therapy by extended release of timolol from nanoparticle loaded silicone-hydrogel contact lenses," J. Controlled Release, 165, 82–89, (2013).

Jung, H.J., and A. Chauhan, "Temperature sensitive contact lenses for triggered ophthalmic drug delivery," Biomaterials, 33, 2289-2300 (2012).

Kapoor, Y., J. C. Thomas, G. Tan, V.T. John, A. Chauhan, "Surfactant-laden soft contact lenses for extended delivery of ophthalmic drugs," Biomaterials, 30, 867-878 (2009).

Karlgard, C.C., L.W. Jones, C. Moresoli, "Ciprofloxacin interaction with silicon-based and conventional hydrogel contact lenses," Eye Contact Lens, 29, 83–89, (2003b).

Karlgard, C.C., N.S. Wong, L.W. Jones, C. Moresoli, "In vitro uptake and release studies of ocular pharmaceutical agents by silicon-containing and p-HEMA hydrogel contact lens materials," Int. J. Pharm., 257, 141–151 (2003a).

Katarina, E., C. Johan, P. Roger, "Rheological evaluation of poloxamer as an in situ gel for ophthalmic use," Eur. J. Pharm. Sci. 6 105–112 (1998).

Klein, B.E., R. Klein, K.E. Lee, "Heritability of risk factors for primary open-angle glaucoma: the Beaver Dam Eye Study," Invest. Ophthalmol. Vis. Sci., 45, 59-62 (2004).

Kohane, D.S. "Microparticles and nanoparticles for drug delivery," Biotechnol. Bioeng., 96, 203-209 (2007).

Korogiannaki, M. "Extended ocular drug delivery using hyaluronic acid-containing model silicone hydrogel materials," Open Access Dissertations and Theses. Paper 7616 (2013).

Kortesuo, P., M. Ahola, M. Kangas, A. Yli-Urpo, J. Kiesvaara, and M. Marvola, "In vitro release of dexmedetomidine from silica xerogel monoliths: effect of sol-gel synthesis parameters," Int. J. Pharm., 221, 107-114 (2001a).

Kortesuo, P., M. Ahola, M. Kangas T. Leino, S. Laakso, L. Vuorilehto A. Yli-Urpo, J. Kiesvaara, M. Marvola, "Alkyl-substituted silica gel as a carrier in the controlled release of dexmedetomidine," J. Controlled Release, 76, 227-238 (2001b).

Landfester, K. and V. Mailänder, "Nanocapsules with specific targeting and release properties using miniemulsion polymerization," Expert Opin. Drug Deliv., 10, 593-609 (2013).

Landfester, K., F. Tiarks, H.-P. Hentze, and M. Antonietti, "Polyaddition in miniemulsions: A new route to polymer dispersions," Macromol. Chem. Phys., 201, 1-5 (2000).

Law, S.K. and D.A. Lee, "Ocular Pharmacology," In P. A. Netland (Ed.), *Glaucoma Medical Therapy Principles and Management*. (2nd ed.). (pp 1-16). New York, NY: Oxford University Press (2008).

Lawrence, M.J. and G.D. Rees, "Microemulsion-based media as novel drug delivery systems," Adv. Drug Delivery Rev., 64, 175-193 (2012).

Le Bourlais, C., L. Acar, H. Zia, P.A. Sado, T. Needham, R. Leverge, "Ophthalmic drug delivery systems", Prog. Retin. Eye Res. 17, 33–58 (1998).

Lee, D.A., and E. Higginbotham, "Glaucoma and its treatment: a review," Am J Health-Syst. Pharm., 62, 691-699 (2005).

Li, C.C., and A. Chauhan, "Modeling ophthalmic drug delivery by soaked contact lenses," Ind. Eng. Chem. Res., 45, 3718–3734 (2006).

Li, C-C., Abrahamson, M., Kapoor, Y., and Chauhan, A., "Timolol transport from microemulsions trapped in HEMA gels," J. Colloid and Interface Sci., 315, 297-306 (2007).

Liu, L. and H. Sheardown, "Glucose permeable poly (dimethyl siloxane) poly (N-isopropylacrylamide) interpenetrating networks as ophthalmic biomaterials," Biomaterials, 26, 233-244 (2005).

Lorenz, M.R. M-V. Kohnle, M. Dass, P. Walther, A. Hocherl, U. Ziener, K. Landfester, V. Mailänder, "Synthesis of fluorescent polyisoprene nanoparticles and their uptake into various cells," Macromol. Biosci., 8, 711-727 (2008).

Lu, C., A.S. Mikhail, X. Wang, M.A. Brook, and C. Allen, “Hydrogels containing core cross-linked block co-polymer micelles,” J. Biomat. Sci.- Polym. E., 23, 1069-1090 (2012).

Lu, C., Yoganathan, R.B., Kociolek, M., and C. Allen, “Hydrogel containing silica shell cross-linked micelles for ocular drug delivery,” J. Pharm. Sci., 102, 627-637 (2013).

Ma, W.D, H. Xu, C. Wang, S.F. Nie, W.S. Pam, “Pluronic F127-g-poly(acrylic acid) copolymers as in situ gelling vehicle for ophthalmic drug delivery system,” Int. J. Pharm. 350, 247–256 (2008).

Malam, Y., M. Loizidou, A.M. Seifalian, “Liposomes and nanoparticles: nanosized vehicles for drug delivery in cancer,” Trends Pharmacol. Sci., 30, 592-599 (2009).

Mateen, R., "Cyclodextrin-functionalized microgels and injectable hydrogels for the delivery of hydrophobic drugs," Open Access Dissertations and Theses. Paper 6553 (2012).

McNamara, N.A., K.A. Polse, R.D. Brand, A.D. Graham, J.S. Chan, C.D, McKenney, Tear mixing under a soft contact lens: effects of lens diameter,” Am. J. Ophthalmol., 127, 659-665 (1999).

Medline Plus, “Dexamethasone oral.” 2010.

Medline Plus, “Dexamethasone ophthalmic.” 2010.

Medline Plus, “Acetazolamide.” 2010.

Medline Plus, “Atropine.” 2011.

Merck Canada Inc., “Timoptic-XE: timolol maleate ophthalmic gellan solution product monograph,” (2013)

The Merck Index, 14th Ed., “Dexamethasone; monograph number 02943,” Perkin Elmer (2006).

Moriguchi, I. S. Hirono, I. Nakagome, and H. Hirano, “Comparison of reliability of log P values for drugs calculated by several methods. Chem. Pharm. Bull., 42, 976-978 (1994).

Moorthy, R.S, A. Mermoud, G. Baerveldt, D.S. Minckler, P.P. Lee, N.A. Rao., “Glaucoma associated with uveitis,” Surv. Ophthalmol., 41, 361-394(1997).

Muztar, J., Chari, G., Bhat, R., Ramarao, S., and Vidyasagar, D., "A high-performance liquid chromatographic procedure for the separation of cocaine and some of its metabolites from acepromazine, ketamine, and atropine from serum," J. Liq. Chromatogr., 18, 2635-2645 (2006).

Netland, P.A., T. Landry, E.K. Sullivan, R. Andrew, L. Silver, A. Weiner, S. Mallick, J. Dickerson, M.V.W. Bergamini, S.M. Robertson, A.A. Davis, The Travoprost study group, "Travoprost compared with latanoprost and timolol in patients with open-angle glaucoma or ocular hypertension," Am. J. Ophthalmol. 132, 472–484(2001).

Paiphansiri, U., P. Tangboriboonrat, K. Landfester, "Polymeric nanocapsules containing an antiseptic agent obtained by controlled nanoprecipitation onto water-in-oil miniemulsion droplets," Macromol. Biosci., 6, 33-40 (2006).

Pang, H., S. Zhou, L. Wu, M. Chen and G. Gu, "Fabrication of silicone oil microcapsules with silica shell by miniemulsion method," Colloids Surf., A. 364, 42-48 (2010).

Parasrampuria, J. In: Brittain HG, editor. Analytical profiles of drug substances and excipients. Vol. 22 San Diego, London: Academic Press. pp 3–32 (1993).

Park, S.J and K.S. Kim, "Influence of hydrophobe on the release behaviour of vinyl acetate miniemulsion polymerization," Colloids Surf., B. 46, 52-56 (2005).

Pope, E.J.A., K. Braun, and C.M. Peterson, "Bioartificial organs I: silica gel encapsulated pancreatic islets for the treatment of diabetes mellitus," J. Sol-Gel Sci. Technol., 8, 635-639 (1997).

Radziuk, D., A. Skirtach, G. Sukhorukov, D. Shchukin, H. Mohwald, "Stabilization of silver nanoparticles by polyelectrolytes and poly(ethylene glycol)." Macromol. Rapid Commun. 27, 848-855 (2007).

Remko, M., and C-W. von der Lieth, "Theoretical study of gas-phase acidity, pKa, lipophilicity, and solubility of some biologically active sulfonamides." Bioorg. Med. Chem. 12, 5395–5403 (2004).

Sherwood, M. J. Brandt, "Six-month comparison of bimatoprost once-daily and twice-daily with timolol twice-daily in patients with elevated intraocular pressure. Surv. Ophthalmol. 45 (Suppl 4): S361-S368 (2001).

Schultz, C., J. Breaux, J. Schentag, D. Morck, "Drug delivery to the posterior segment of the eye through hydrogel contact lenses," Clin. Exp. Optom., 94, 212–218 (2011).

Shih, Y.F., C.K. Hsiao, C.J. Chen, C.W. Chang, P.T. Hung, and L.L. Lin, "An intervention trial on efficacy of atropine and multi-focal glasses in controlling myopic progression," Acta. Ophthalmol. Scand., 79, 233-236 (2001).

Siddique, S.S., A.M. Suelves, U.Baheti, C. S. Foster, "Uveitis and glaucoma," Surv. Ophthalmol. 58, 1-10 (2013).

Soluri, A. A. Hui, L. Jones, "Delivery of KetotifenFumarate by Commercial Contact Lens Materials," Optom. Vis. Sci. 89, 1140–1149 (2012).

Srividya, B, and R.M. Cardoza, "Sustained ophthalmic delivery of ofloxacin from a pH triggered in situ gelling system", J. Controlled Release. 73, 205–211 (2001).

Tighe, B., "Silicone hydrogels: structure, properties and behaviour," In D. F. Sweeney (Ed.), *Silicone Hydrogels Continuous Wear Contact Lenses* (2nd ed.). (pp 1-27). Edinburgh: Butterworth Heinemann (2004).

Tong, L., X.L. Huang, A.L.T. Koh, X. Zhang, D.T.H. Tan, and W.-H. Chua, "Atropine for the treatment of childhood myopia: effect on myopia progression after cessation of atropine," Ophthalmology. 116, 572-579 (2009).

Tran, V-T, J-P. Benoit, M-C. Venier-Julienne, "Why and how to prepare biodegradable, monodispersed, polymeric microparticles in the field of pharmacy?" Int. J. Pharm. 407, 1-11 (2011).

Underhill, R.S, A.V. Jovanovic, S.R. Carino, M. Varshney, D.O. Shah, D.M. Dennis, T.E. Morey, R.S., Duran, "Oil-filled silica nanocapsules for lipophilic drug uptake: implications for drug detoxification therapy," Chem. Mater. 14, 4919-4925 (2002).

Urtti, A., "Challenges and obstacles of ocular pharmacokinetics and drug delivery," Adv. Drug Delivery Rev. 58, 1131-1135 (2006).

Vandamme, T.F, "Microemulsions as ocular drug delivery systems: recent developments and future challenges," Prog. Retin. Eye Res. 21, 15–34 (2002).

van der Valk, R. C.A.B. Webers, J.S.A.G. Schouten, M.P. Zeeger, F. Hendrikse, M.H. Prins, "Intraocular pressure–lowering effects of all commonly used glaucoma drugs: a meta-analysis of randomized clinical trials," Ophthalmology. 112, 1177–1185 (2005).

Vasantha, R.S.P. and R.K. Panduranga, "Collagen ophthalmic inserts for pilocarpine drug delivery systems", Int. J. Pharm. 47, 95–102 (1988).

Wajs, G. and J.C. Meslard, “Release of therapeutic agents from contact lenses,” Crit. Rev. Ther. Drug. 2, 275–289 (1986).

Wang, N., H. Wu, and Z. Fan, “Primary angle closure glaucoma in Chinese and Western populations,” Chin. Med. J., 115, 1706-1715 *(*2002).

Xiong, W., X. Gao, Y. Zhao, H. Xu, and X. Yang, “The dual temperature/pH-sensitive multiphase behavior of poly(N-isopropylacrylamide-co-acrylic acid) microgels for potential application in in situ gelling system”, Colloids Surf., B. 84 103–110 (2011).

Yakushiji, T., K. Sakai, A. Kikuchi, T. Aoyagi, Y. Sakurai, and T. Okano, “Effects of Cross-Linked Structure on Temperature-Responsive Hydrophobic Interaction of Poly(N-isopropylacrylamide) Hydrogel-Modified Surfaces with Steroids,” Anal. Chem. 71, 1125-1130 (1999).

Appendix A

Table A1. Reagents and source

Reagent	Source
1.0 M HCl	EBD Chemicals
1.0 M NaOH	EBD Chemicals
1x PBS	Biorad
Acetazolamide	Sigma-Aldrich
Atropine	Sigma-Aldrich
Dexamethasone	Sigma-Aldrich
DMA	Sigma-Aldrich
DMS-PEO	Gelest
EGDMA	Sigma-Aldrich
Ethyl butyrate	Sigma-Aldrich
HEMA	Sigma-Aldrich
IPM	Sigma-Aldrich
MATO	Gelest
OTMS	Sigma-Aldrich
SDS	Sigma-Aldrich
Soybean oil	Sigma-Aldrich
TEOS	Sigma-Aldrich
Triacetin	Sigma-Aldrich
TRIS	Gelest
TRIS-OH	Gelest
Triton X-100	Sigma-Aldrich

Table A2. Recipe for 1x PBS

Chemical	Molecular weight (g/mol)	Concentration (g/L)	Concentration (mol/L)
Potassium chloride	74.55	0.20	0.003
Potassium phosphate monobasic	136.09	0.24	0.002
Sodium chloride	58.44	8.00	0.137
Sodium phosphate heptahydrate	268.07	2.68	0.010

Appendix B

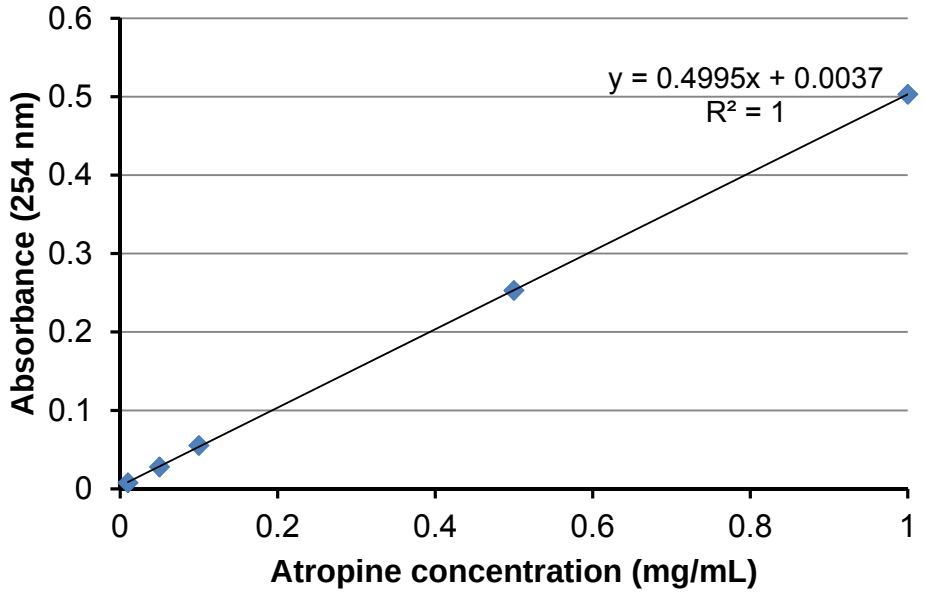

Figure A1. Calibration curve of atropine in PBS. Absorbance measured at 254 nm. Data are the mean (± SD) for three repeat measurements.

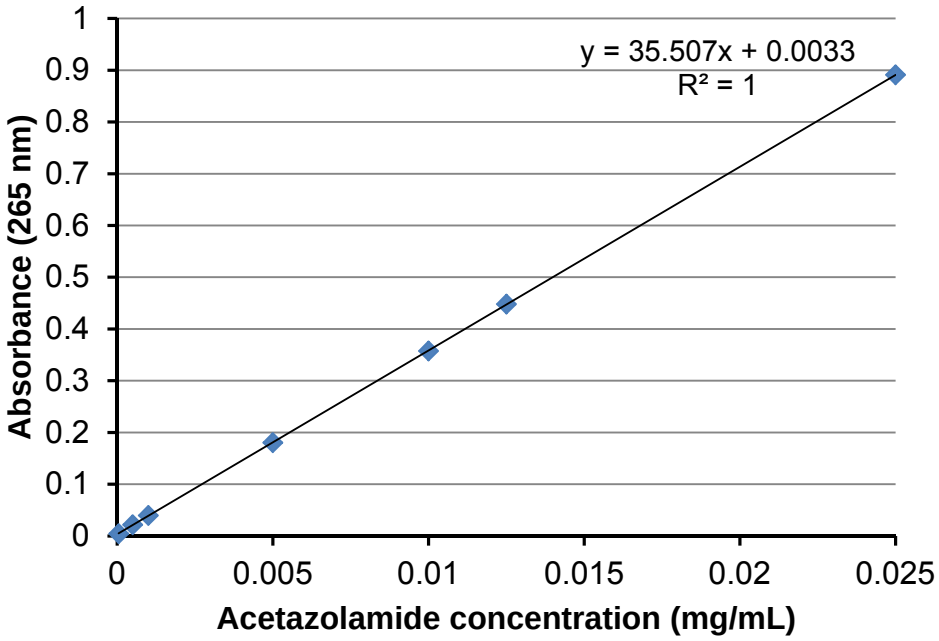

Figure A2. Calibration curve of acetazolamide in PBS. Absorbance measured at 265 nm. Data are the mean (± SD) for three repeat measurements.

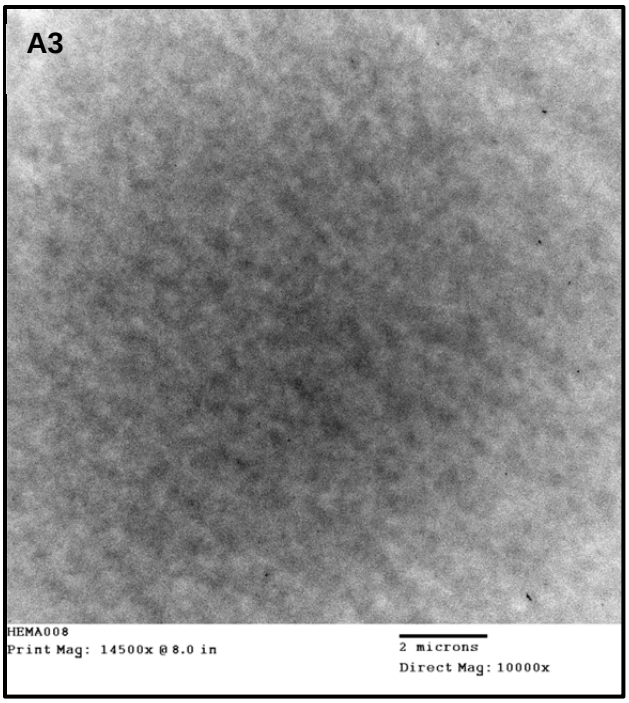

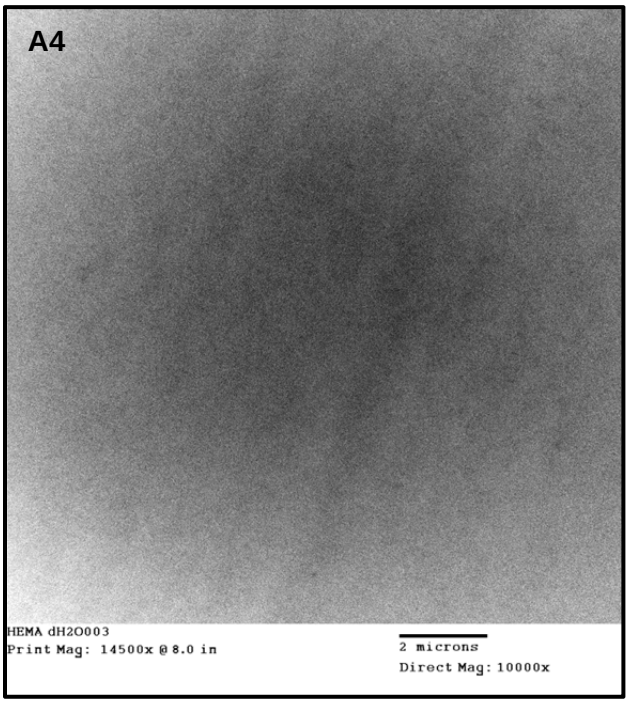

Figure (A3). TEM micrograph of HEMA and **(A4).** TEM micrograph of HEMA/dH_2O hydrogel at 10,000x magnification. Scale bar is 2 μm.